Published in "Journal of Anatomy 233(5): 644–665, 2018"
which should be cited to refer to this work.

Post-metamorphic ontogeny of *Zoroaster fulgens* Thomson, 1873 (Asteroidea, Forcipulatacea)

Marine Fau[1] and Loïc Villier[2]

[1]*Department of Geosciences, University of Fribourg, Fribourg, Switzerland*
[2]*Centre de Recherche sur la Paléobiodiversité et les Paléoenvironnements, Sorbonne Université, Paris, France*

Abstract

The complete ontogenetic development of an asteroid skeleton has never been described formally for any species. Here, we describe in detail the post-metamorphic ontogeny of *Zoroaster fulgens* Thomson, 1873. The major novelty of our work is the description of patterns of plate addition, the ontogeny of the internal ossicles, as well as the variability of ossicles according to their position along series. Seven specimens collected in the Rockall Basin (North Atlantic) were dissected with bleach and their anatomy was documented using a scanning electron microscope. The external anatomy was additionally observed on more than 30 specimens. We found that the overall structure of the skeleton does not change much between juveniles and adults, but the shape of individual ossicle changes during growth. Allometric scaling was particularly visible on the orals, ambulacrals and adambulacrals. The shape of an ossicle is more dependent of its position along the arm series than of its individual size. Many morphological features differentiate progressively during ontogeny, while others are expressed consistently among specimens. The study of this ontogenetic series allows discussing the homology between the structures present on the ossicles of *Z. fulgens* in particular and other forcipulatacean sea stars in general (i.e. muscles insertions and articulation areas). The new data obtained in this study provide a comprehensive framework of the anatomy and ontogeny of *Z. fulgens* that will help resolve taxonomic and phylogenetic controversies in the future.

Key words: Asteroidea; echinoderms; ontogeny; ossicles; skeleton.

Introduction

Asteroidea (sea stars or starfish) is one of the five extant clades of Echinodermata, which is otherwise comprised of Echinoidea (sea urchins), Holothuroidea (sea cucumbers), Ophiuroidea (brittle stars, basket stars) and Crinoidea (sea lilies and feather stars; Janies, 2001; Telford et al. 2014). One of the characteristic features of echinoderms is their mesodermal skeleton, which is made of ossicles articulated via mutable connective tissues and muscles (Blowes et al. 2017). The ossicles are differentiated according to their anatomical position and function. The structure of the asteroid's skeleton has been studied since the late 19th century, mainly for taxonomic purposes (Cuénot, 1887; Turner & Dearborn, 1972). Eight principal types of ossicles are recognized, of which most are serially organized along the axes of the arms. The body shape and architecture, the number of ossicle series and their articulation allow diagnosing the main groups of asteroids (Blake, 1987; Gale, 1987a; Mah & Blake, 2012). The structure of the skeleton and the accessory elements (granules, spines, sclerites, pedicellariae) provide the basis for numerous characters with which extant and extinct species are diagnosed and that can help in phylogenetic reconstruction (Blake & Hagdorn, 2003; Villier et al. 2004; Mah, 2006, 2007; Mah et al. 2010, 2015; Gale, 2011).

Over the course of the 20th century, a series of palaeontologists developed a taxonomic practice based on isolated asteroid skeletal elements found in sediments (Spencer, 1913; Rasmussen, 1950; Müller, 1961; Blake, 1972; Gale, 1987b, 1988; Breton, 1992). This approach has since been validated by internal consistency and repeatability (Breton, 1995; Villier et al. 2004), but requires a precise understanding of asteroid skeletons and a strong background in the comparative anatomy of ossicles. The fine anatomy of ossicles reveals muscle insertions, faces for articulation with adjoining ossicles, tubercles and pits for insertion of accessories (e.g. spines, granules), as well as grooves, cavities or bosses that serve as guides for soft organs (Turner & Dearborn, 1972; Blake, 1976; Gale, 2011). The potential phylogenetic signal contained within the anatomy of isolated ossicles has only been explored recently (Blake, 1987; Gale,

Correspondence
Marine Fau, Université de Fribourg, Department of Geosciences, Chemin du musée, 6, 1700 Fribourg, Switzerland. E: marine.fau@unifr.ch

1987a, 2011; Blake & Elliott, 2003; Villier et al. 2004). However, a reliable framework for comparative anatomy cannot be achieved pending exploration of intraspecific, individual and ontogenetic variability of each ossicle type. The skeleton of a juvenile asteroid starts its development at the end of the larval stage (Fewkes, 1888; Mortensen, 1921; Gordon, 1929). The early development of the skeleton, including the order of ossicle differentiation and the dynamics of serial plate addition, is documented for several groups (Fewkes, 1888; Gemmill, 1912, 1914, 1920; Komatsu, 1975; Komatsu et al. 1979; Siddall, 1979; Komatsu & Nojima, 1985; Sumida et al. 2001; Lopes & Ventura, 2016). Different ossicle types grow following distinct patterns. Although the ossicles forming the oral frame (mouth angle ossicles or orals, first ambulacrals and odontophores), the primary ossicles of the disc (central plate, primary interradials, primary radials and madreporite) and those found at the extremity of each arm (terminals) are fixed in number, their shape, proportion and topological relationships may vary during growth (Mooi et al. 1998; Hotchkiss, 2009). All other ossicle types increase both in number and in size during ontogeny. The ossicles that form the ambulacral groove (ambulacrals and adambulacrals) as well as the principal ossicles forming the body frame (marginals and carinals, when present) are added serially at the tip of the arms. The ossicles of the oral (actinal) and dorsal (abactinal) faces express more variable pattern of development (Mooi & David, 2000).

Each echinoderm ossicle is made up of a three-dimensional meshwork of high-magnesium calcite called stereom (Raup, 1966). Stereom grows by secretion of amorphous calcium carbonate that transforms progressively to calcite when no longer maintained biologically (Ameye et al. 2001). The stereom meshwork is in constant change during ossicle development and adapts to functional constraints (Smith, 1980; Dubois & Chen, 1989). The ontogeny of individual ossicles remains poorly studied *in vivo* and is usually investigated through comparison of ossicles from individuals of different size. Palaeontologists explored the evolution of the marginal plates of goniasterid asteroids (Müller, 1961; Gale, 1987a, 1988; Breton, 1992, 1995), but virtually no data are available for the other ossicle types and other groups of Asteroidea.

The goal of the present paper is the description of the ontogeny of a single species of asteroid from a juvenile to an adult stage, including skeletal architecture, skeletal arrangement as well as growth patterns for all types of ossicles. The analysis focuses on the only species of the genus *Zoroaster* that is present in the Atlantic, *Zoroaster fulgens* Thomson, 1873. Ossicle growth and anatomy are primarily based on seven specimens representing a growth series.

The genus *Zoroaster* and the family Zoroasteridae are of major importance for understanding asteroid phylogeny, because Zorasteridae is thought to be the sister group of the rest of Forcipulatacea, a hypothesis supported by both molecular and morphological data (Mah, 2000; Gale, 2011; Mah & Foltz, 2011a). A precise understanding of the ontogeny and comparative anatomy of *Z. fulgens* is therefore expected to provide new insights that may help resolve internal relationships within Forcipulatacea.

Materials and methods

Biological material

Many nominal species of *Zoroaster* initially described from the Atlantic (e.g. *Zoroaster ackleyi* Perrier, 1881; *Zoroaster diomedae* Verrill, 1884; *Zoroaster longicauda* Perrier, 1885; *Zoroaster trispinosus* Koehler, 1896) have been synonymized with *Z. fulgens* in the past decades because obvious morphological differences are lacking (Downey, 1970; Clark & Downey, 1992; Mah, 2007). However, Howell et al. (2004) recently suspected the three morphotypes (i.e. 'robust', 'slender' and 'long-arms') of *Z. fulgens* found in the Porcupine Seabight (North Atlantic) to represent three potential cryptic species. The distribution of these morphotypes depends on depth, and reproductive isolation is suggested by the molecular data (Howell et al. 2004). A taxonomic revision of the species is therefore needed. In order to limit taxonomic bias, all specimens selected for this study can be attributed to the 'slender-arm' morphotype (*sensu* Howell et al. 2004), and were collected from a limited area and depth range in the Rockall Basin. Seven specimens from the Muséum National d'Histoire Naturelle (MNHN, Paris, France) were selected that document the ontogeny of *Z. fulgens* from juvenile to adult. To ease reading, we used the letter 'Z' followed by a number from 1 to 7 to refer to these specimens, Z1 being the smallest specimen and Z7 the largest (see Table 1 for measurements and collection numbers). The six juvenile specimens (Z1–Z6) together with 24 measured juveniles (MNHN-IE-2016-563 to MNHN-IE-2016-586) come from a batch (MNHN-IE-2013-12853) collected during the INCAL expedition in 1976. The adult (Z7) was collected during the expedition NORATLANTE-3 in 1969.

Sumida et al. (2001) described early post-metamorphic stages of *Z. fulgens* from several specimens ranging from $R = 0.53$ to $R = 3.75$ mm in diameter. Their illustrations are taken as reference for the description of the earliest stages of ontogeny.

In order to compare the characters observed on *Z. fulgens* with other forcipulatacean asteroids, three specimens belonging to other Forcipulatacea were selected and dissected (from the MNHN and the Yale Peabody Museum, YPM): the asteriid *Pisaster ochraceus* (Brandt, 1835; YPM 87690), the brisingid *Brisingaster robillardi* de Loriol, 1883 (MNHN-IE-2013-12874) and the stichasterid *Neomorphaster forcipatus* Verrill, 1894 (YPM 87682).

Dissections

Specimens were prepared by immersion in a dilute solution of sodium hypochlorite (bleach), followed by rinsing with tap water, drying, mounting and gold coating (60–100 nm) on a scanning electron microscope (SEM) stub. The samples were SEM imaged using a Hitachi TM3000 (Centre de Recherche sur la Paléobiodiversité et les Paléoenvironnements, Paris, France) and a FEI XL30 Sirion FEG (Université de Fribourg, Switzerland).

Ossicles were measured from the SEM images using the software Image J. Measurements were then log transformed to explore allometric scaling (Kerkhoff & Enquist, 2009).

Table 1 List of the dissected specimens.

Collection number	Specimen code	Number of individuals	*R* (mm)	*r* (mm)	Coordinates	Depth (m)
IE-2014-642	Z1	1	12	2	56°33′N 11°11′W	2483
IE-2014-643	Z2	1	15	3	56°33′N 11°11′W	2483
IE-2014-644	Z3	1	18	3	56°33′N 11°11′W	2483
IE-2014-645	Z4	1	26	4	56°33′N 11°11′W	2483
IE-2014-646	Z5	1	36	4	56°33′N 11°11′W	2483
IE-2013-12854	Z6	1	66	6	56°33′N 11°11′W	2483
IE-2014-647	Z7	1	114	14	52°06′N 12°38′W	2215
IE-2016-563 to IE-2016-586	–	24	–	–	56°33′N 11°11′W	2483
IE-2013-12853	–	> 100	–	–	56°33′N 11°11′W	2483

All *Zoroaster fulgens* are from the Muséum National d'Histoire Naturelle (Paris, France), and are registered with the format MNHN-IE-20XX-XXX. Specimens are coded according to their diameter *R* from the centre of the disc to the tip of the arms (Z1–Z7). The diameter *r* corresponds to the diameter of the disc.

Terminology

We utilized the following anatomical conventions to describe ossicle orientation in the asteroid skeleton: (i) a horizontal plane separating the actinal surface (adoral) from the abactinal surface (aboral); (ii) a radial plane of symmetry that vertically crosses each arm at its centre along the radial vessel, separating surfaces that face towards the radial plane (adradial) from those that face away from this plane (abradial); and (iii) the proximal direction toward the centre of the disc vs. the distal direction toward the tip of the arm.

There have been several historical treatments that have been proposed to describe the ossicles of asteroids (Turner & Dearborn, 1972; Blake, 1973; Gale, 2011). Here, nomenclature mostly follows Gale (2011), with some modification and addition of formally unnamed structures. Table 2 summarizes all anatomical terms and abbreviations used herein, including their equivalent in Gale (2011). These abbreviations are highlighted in the text through the use of italics.

Results

Disc

The disc is composed of five radial and five interradial plates arranged in a circle, a variable number of abactinal plates set around the central plate inside the circle of radials and interradials, and the madreporite, which is linked with an interradial (Fig. 1). For specimens smaller than $R = 2.04$ mm, the disc is mainly composed of the central plate and of the five interradials, all of them bearing one central primary spine. Although radials are present in these specimens, they are small and the interradials therefore are in contact with each other (Fig. 1A). In specimens larger than $R = 2.04$ mm, the relative size of the radials increases until they become prominent plates of the disc and fully separate the interradials from one another (Fig. 1A–C). Sumida et al. (2001) did not mention the occurrence of a madreporite in the earliest ontogenetic stages.

The madreporite is present in all analysed specimens, even the smallest ones (Z1, Fig. 1B). The madreporite is relatively small compared with the radials and interradials, and round with sharply tapering edges (Fig. 2C). It is not fused with but inserts inside a cavity formed by the adjacent interradials (Fig. 2A,B). A similar cavity is absent on the four remaining interradials (Fig. 2E). The interradials overlap the abactinals distally and proximately (Fig. 1B,C), but are overlapped by the radials on their lateral sides on the articular facet (*ria*; Fig. 2A,E,F). Radials are overlapped distally by the first plate of the carinal series on the articulation area *cra* (Fig. 2F). A notch along one side of the central plate marks the anus location (Figs 1B,C and 2D).

The disc does not grow as much as the arm grows in length. Only a few abactinals appear around the central plate, inside the circle formed by the primary radials and interradials. As the central, interradial and radial plates grow larger, their shapes remain constant. The madreporite develops isometrically with its associated interradial, but its shape and position remain constant (Fig. 1A–C).

Terminal plates

Two measures were taken on the terminals: the maximum length (L_{max}) corresponds to the length of the terminal from the distal edge to the proximal edge; and the minimum length (L_{min}) corresponds to the length from the distal edge to the centre of the notch (Table 3).

Right after metamorphosis the terminals are robust with a convex distal edge and a rather straight proximal edge. At $R = 0.58$ mm, there is no differentiation of the disc and the arms because of the absence of primary radial plates. The terminals delineate most of the body outline, and they represent half of the specimen's diameter ($L_{max}/R = 48.28\%$; Table 3). At $R = 1.05$ mm, the shape of the terminals does not change, they still contribute for half of the radius (Table 3), but radial plates are forming thereby pushing the terminals distally to form short arms. The proximal edge of the terminals becomes concave in the specimen $R = 1.59$ mm. From this size, the proximal notch opens deeper (L_{min}/L_{max} decrease) until reaching a maximum depth of

Table 2 List of the terms and abbreviations used in this paper.

Terms/ abbreviation	Gale (2011)	Definition
1st podial basin	1st tf	On the oral ossicle, area between the proximal and the distal process where the first tube feet lie. Generally associated with denser and flatter stereom
abiim		Interoral abactinal muscle
abtam		Transverse abactinal interambulacral muscle
aciim		Interoral actinal muscle
actam		Transverse actinal interambulacral muscle
base (of the ambulacrals)		Actinal part of the ambulacrals, as defined by Gale (2011)
body (of the oral ossicle)	–	Actinal part of the ossicle bearing the spines, the *odom* and *aciim* muscles on the interradial side, and the *iioa* articulation
bump	sos	Spine attachment structure, consists of an articulation area at the top of a bulge
cra	–	Carinal-radial articulation
dada	ada 2, ada 3	Ambulacral/adambulacral articulation (distal on the ambulacral, proximal on the adambulacrals)
dadam		Distal ambulacral/adambulacral muscle, on the ambulacrals
dicoa	dcoa	Trace on the oral plates of the articulation between the oral and the first ambulacral ossicle
dicoam	–	Oral/first ambulacral distal muscle insertion, on the oral
doda		Distal oral/odontophore articulation on the oral
furrow	–	Furrow on the distal process of the first ambulacrals and on the *shaft* of ambulacrals
head (of the ambulacrals)		Abactinal part of the ambulacrals, as defined by Gale (2011)
iia	–	Internal interradial actinals
iioa		Interoral articulation
interada	adada	Interadambulacral articulation
interadam	adadam	Interadambulacral muscle
lia		Longitudinal interambulacral articulation
lim		Longitudinal interambulacral muscle
odom		Odontophore-oral muscle
orada		Oral-adambulacral articulation, on the oral
oradam	oradm	Oral-adambulacral muscle, on the oral
pada	ada1, ada1a, ada1b	Ambulacral-adambulacral articulation (proximal on the ambulacral, distal on the adambulacral)
padam		Proximal ambulacral-adambulacral muscle, on the ambulacral
plateau	–	Flat area at the end of the abactinal *ramus* edge, generally distinct from the latter by a change of slope. Bear the *doda* articulation on the interradial side, and the complex *dicoa*/*dicoam* on the radial side
poda		Proximal odontophore-oral articulation
procoa	pcoa	Proximal oral-first ambulacral articulation, on the orals
procoam	–	Proximal oral-first ambulacral muscle on the oral
pustule	ads, fs, osp	Spine attachment structure, consist of a notch completely or partially surrounded by an articulation area at the top of a bulge
ramus	apo	Abactinal extension of the oral ossicle, bearing the *abiim* muscle and the *poda* articulation on the interradial side, and the complex *procoa*/*procoam* on the radial side of the ossicle. Also called apophyse by Turner & Dearborn (1972), and Gale (2011)
ria	–	Radial-interradial articulation
riom		Interoral muscle
rng		Passageway of the nervous oral ring
rvg		Groove along the oral ossicles in which lies the ring canal of the ambulacral system
shaft (of the ambulacrals)		Middle part of the ambulacrals, as defined by Gale (2011)
Teeth	de	Imbricating teeth and socket structures, on the ambulacral head. Similar structure can appear on the interradial side of the orals and of adambulacrals of the adoral carina
wings	–	Proximal and distal extensions at the *base* of the ambulacral for attachment of the ambulacral/adambulacral muscles (Turner & Dearborn, 1972)

In the second column, abbreviations used by Gale (2011) when they differ, or when the structures were not named (–).

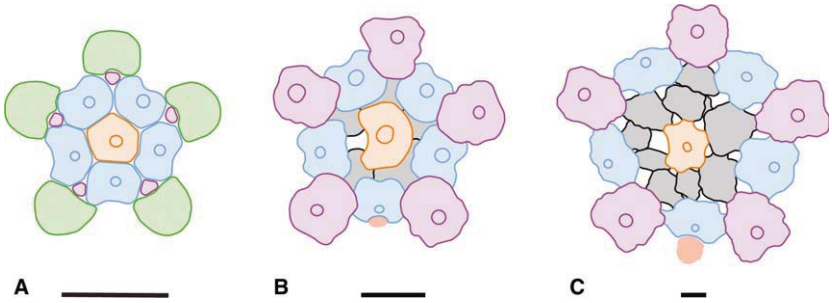

Fig. 1 Evolution of the disc during ontogeny. (A) Disc after metamorphosis, $R = 1.05$ mm, modified from Sumida et al. (2001); (B) disc of Z1; (C) disc of Z7. Coloured areas indicate ossicle homology. In orange: central plates; in grey: abactinal plates; in blue: interradial plates; in purple: radial plates; in green: terminal plates; in red: madreporites. Scale bars: 500 μm.

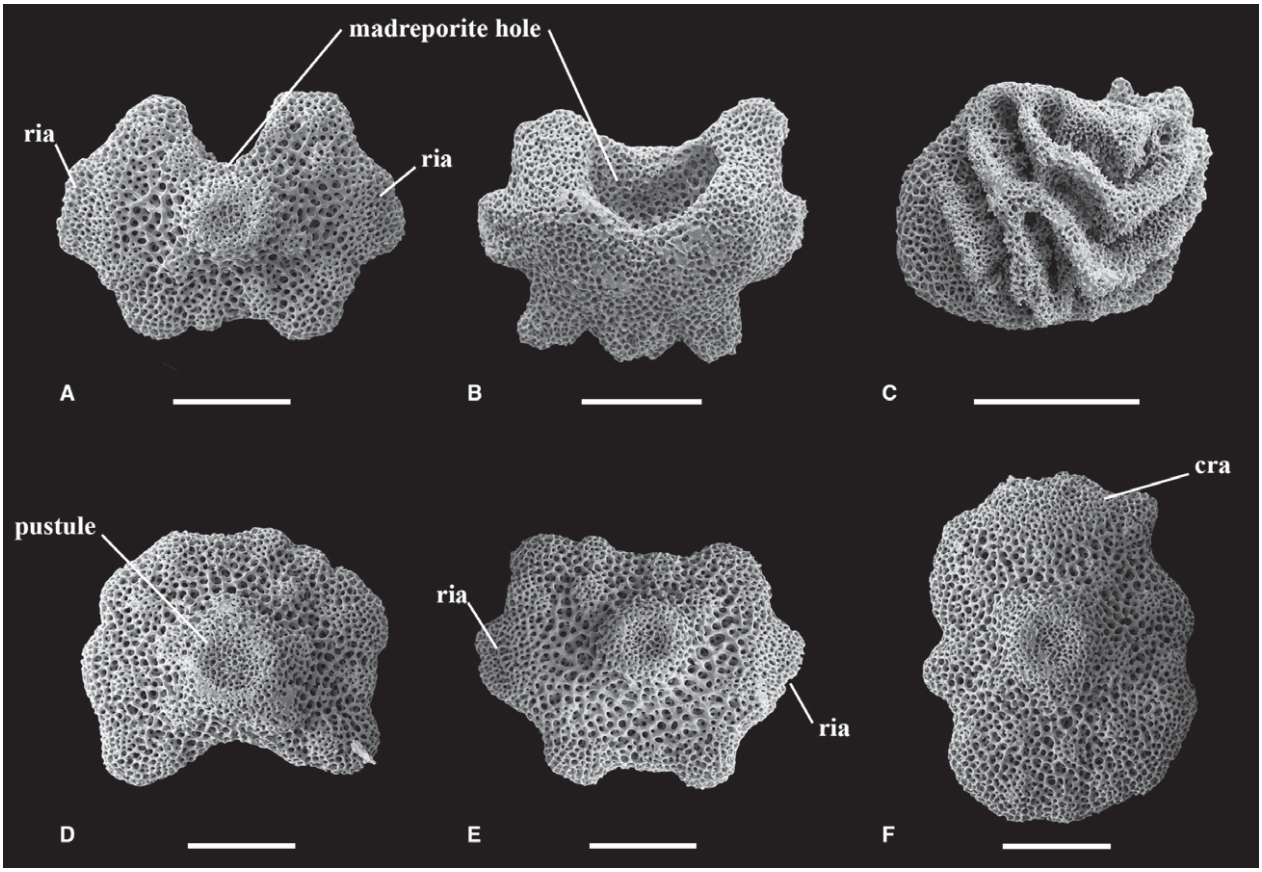

Fig. 2 Scanning electron microscopy (SEM) images of the plates composing the disc. (A) Interradial plate of Z1, in abactinal view; (B) interradial plate of Z3, in actinal view; (C) madreporite of Z5, in abactinal view; (D–F) central, interradial and radial plate of Z1, in actinal view. See Table 2 for abbreviations. Scale bars: 500 μm.

951 μm in specimen Z4. The proximal notch is occupied by newly formed carinals (Fig. 3A–C,L). The notch is progressively reduced on the bigger specimens (Fig. 3B,C; Table 3). The contribution of the terminal to arm length decreases during growth until it represents no more than 1.45% of the *R* in adult forms (Table 3).

Wall skeleton (carinals, abactinals, marginals and actinals)

The arm keeps a similar arrangement of ossicles from juvenile to adult stages. From the central abactinal series to the lateral surface, each arm is composed of a unique row of carinals, one row of abactinals (also called adradials), one row of marginals, several rows of actinals, one row of adambulacral and one of ambulacrals. The marginal row is easily identified because it overlaps both the actinals and abactinals (see discussion regarding the number of marginal rows in Zoroasteridae). The number of actinal rows varies depending on the size of the individual and the position along the arm (Figs 3L,M and 4). Each type of ossicles of the wall skeleton keeps a similar shape during ontogeny (Figs 3D–K and 4). All the actinals, marginals and carinals bear one primary spine each (i.e. spine attached on a *pustule*; Fig. 3D,E,G,I–K). Each actinal, marginal and abactinal possesses four articular facets, whereas the carinals possess

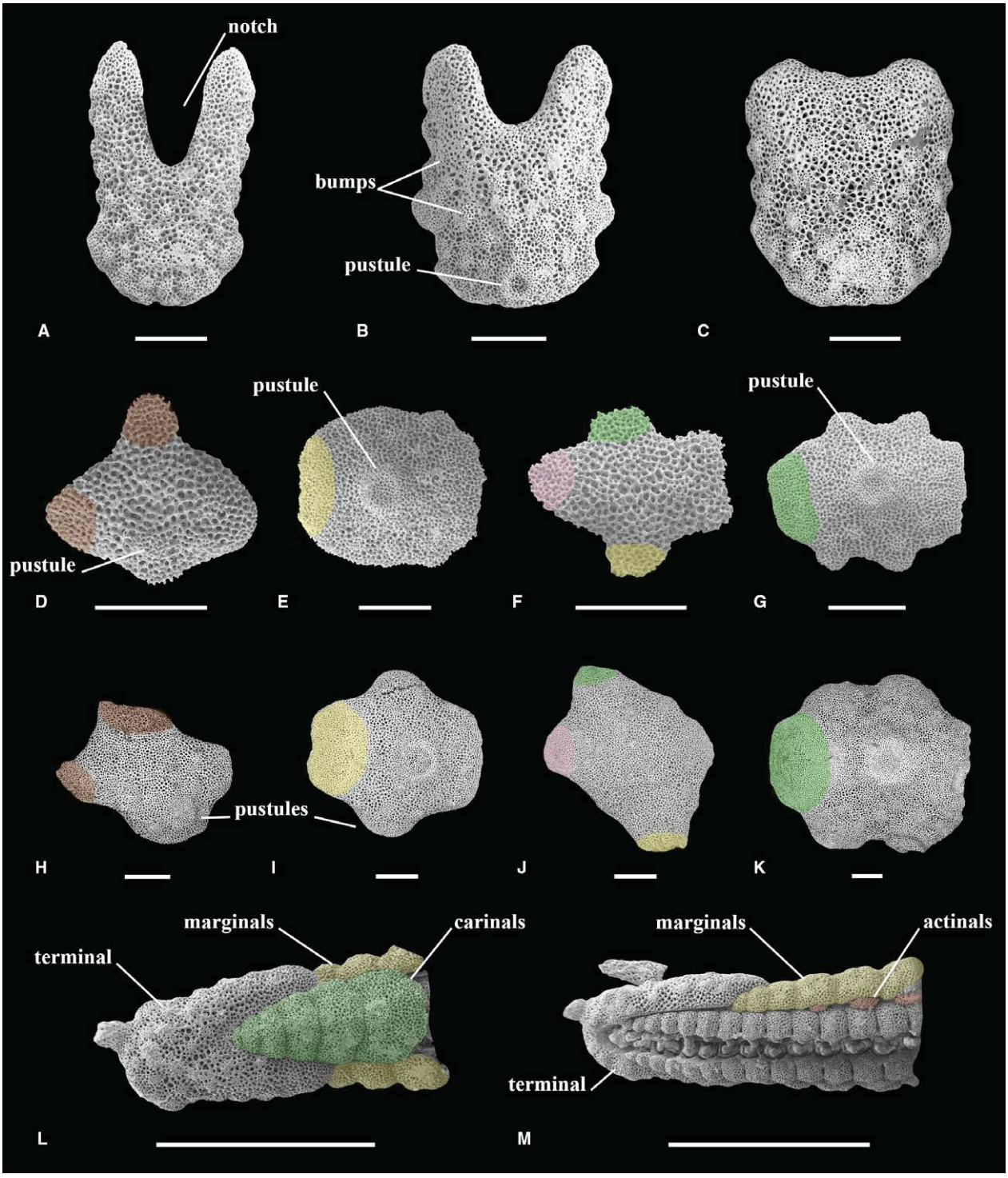

Fig. 3 Scanning electron microscopy (SEM) images of the terminals in abactinal view (A–C) and wall skeleton ossicles in abactinal view (D–M). (A) Terminal of Z3; (B) terminal of Z6; (C) terminal of Z7; (D–G) actinal, marginal, abactinal and carinal of Z1 in this order; (H–K) actinal, marginal, abactinal and carinal of Z7 in this order. In colours, articulation facets covered by other plates: in green: articulation facet covered by carinals; in pink: articulation facet covered by abactinals; in yellow: articulation facet covered by marginals; in brown: articulation facet covered by actinals. Proximal direction to the right, actinal to the bottom. See Table 2 for abbreviations. (L) Abactinal view of one arm of Z1; (M) actino-lateral view of one arm of Z1. In green: carinals; in yellow: marginals; in brown: actinals. Note the presence of only one row of marginals. Proximal direction to the right. Scale bars: 500 μm (A–K); 2 mm (L, M).

Table 3 Measurement of the terminals at different ontogenetic stages.

Specimen	Minimal length (μm)	Maximal length (μm)	L_{min}/L_{max}	Contribution to R (L_{max}/R) (%)
R = 0.58*	–	280	–	48.28
R = 1.05*	–	419	–	53.62
R = 1.59*	553	631	0.876	51.82
R = 2.04*	560	709	0.790	40.69
R = 3.75*	575	888	0.648	29.33
Z1	995	1697	0.586	14.14
Z2	995	1677	0.593	11.18
Z3	930	1747	0.532	9.71
Z4	1078	2029	0.531	7.80
Z5	1260	1986	0.634	5.52
Z6	1212	1690	0.717	2.56
Z7	1601	1657	0.966	1.45

Data for the specimens followed by an asterisk * were taken from the photographs published by Sumida et al. (2001; fig. 11). The length of the terminal is measured in abactinal view, from the distal edge to the edge of the proximal notch (minimal length, L_{min}) and to the tip of the extension (maximal length, L_{max}). The ratio L_{min}/L_{max} characterizes the proximal notch, the smaller the ratio is, the deeper is the notch.

four–six articular facets depending on their relationships to the neighbouring plates (Fig. 3D–K). Every carinal is connected to its proximal and distal neighbour carinals and to two–four abactinals (Fig. 4). The articulation facets develop gradually as lobes during ontogeny, especially in the carinals and marginals. The marginals look blocky on Z2, but they become increasingly cruciform from Z3 to larger specimens (Fig. 3E,I). Actinals appear along the adambulacrals. They are first compressed and flat, with a triangular shape, whereas the older actinals found near the marginals display clearly a cruciform shape with four well-defined lobes (Figs 3D,H,M and 4).

Orals

The articulations *doda* and *poda* are fused on all seven dissected specimens (Fig. 5). The *odom* is a unique muscle insertion on Z1 and Z2 (Fig. 5A,B). Two areas with different stereom types can be distinguished on Z3, but these areas remain in contact (Fig. 5C). The abactinal part (*odom1*) is composed of small, round and regular retiform stereom (*sensu* Smith, 1980), whereas the actinal part (*odom2*) is composed of labyrinthic stereom (*sensu* Smith, 1980). The two parts of the *odom* are lightly separated in Z4, and clearly separated in Z5 and Z6, until they are placed on both sides of the *iioa* on Z7 (Fig. 4D–G). The relative size of the *iioa* increases with growth. The *teeth* differentiate from an initially irregular surface on Z3 (Fig. 5D). The *iioa* occupies most of the *body* of the orals in specimen Z5, and displays regular *teeth*, made of galleried stereom (Fig. 5E–G). Between specimen Z6 and specimen Z7, the general orientation of the ossicle changes to form an angle of about 90° between the *ramus* and the *plateau* (Fig. 5F,G).

On the radial face, the general shape of the ossicle does not change much. The facets for articulation and muscle insertions *procoa*/*procoam*, *dicoa*/*dicoam*, *riom*, *orada* and *oradam* are visible on all studied specimens. Each oral bears two–three spines. A *furrow* appears on Z3 (Fig. 6C) and the stereom of the first podial basin starts to be denser on Z4 (Fig. 6D). The angle between the *body* and the *ramus* decreases between Z5, Z6 and Z7, closing the *rng* (Fig. 6E–G).

First ambulacrals

The first ambulacrals (also called circumoral ossicles) change progressively during growth, with a sequential appearance of characters. The first ambulacrals can be divided into three parts: the head (from the *teeth* to the *actam*); the distal process; and the proximal process.

Teeth are absent on specimen Z1, they appear on Z2, but there is no differentiation until Z4 of the fascicular stereom that compose the *teeth* and the labyrinthic stereom of the rest of the ossicle (Fig. 7A–D). The trace of a *furrow* connected to the oral appears on the proximal process of Z5 (Fig. 7E–G), and a distal *furrow* is visible on the distal process of Z6 and Z7 (Fig. 7F,G). The articulation area *poda*/*doda* is invisible on Z1, Z2 and Z3 (Fig. 7H,J). Traces of galleried stereom are visible at the tip of the distal process

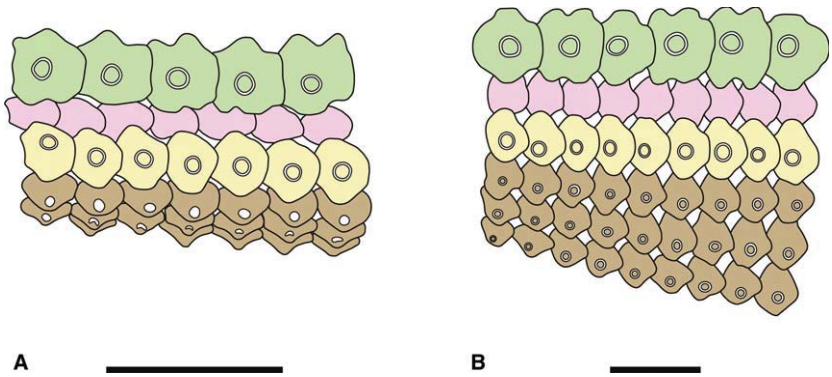

Fig. 4 Reconstruction of plating along the arms. (A) Z6; (B) Z7. Proximal direction to the right, actinal to the bottom. Coloured areas indicate ossicle homology. In green: carinals; in pink: abactinals; in yellow: marginals; in brown: actinals. Scale bars: 5 mm.

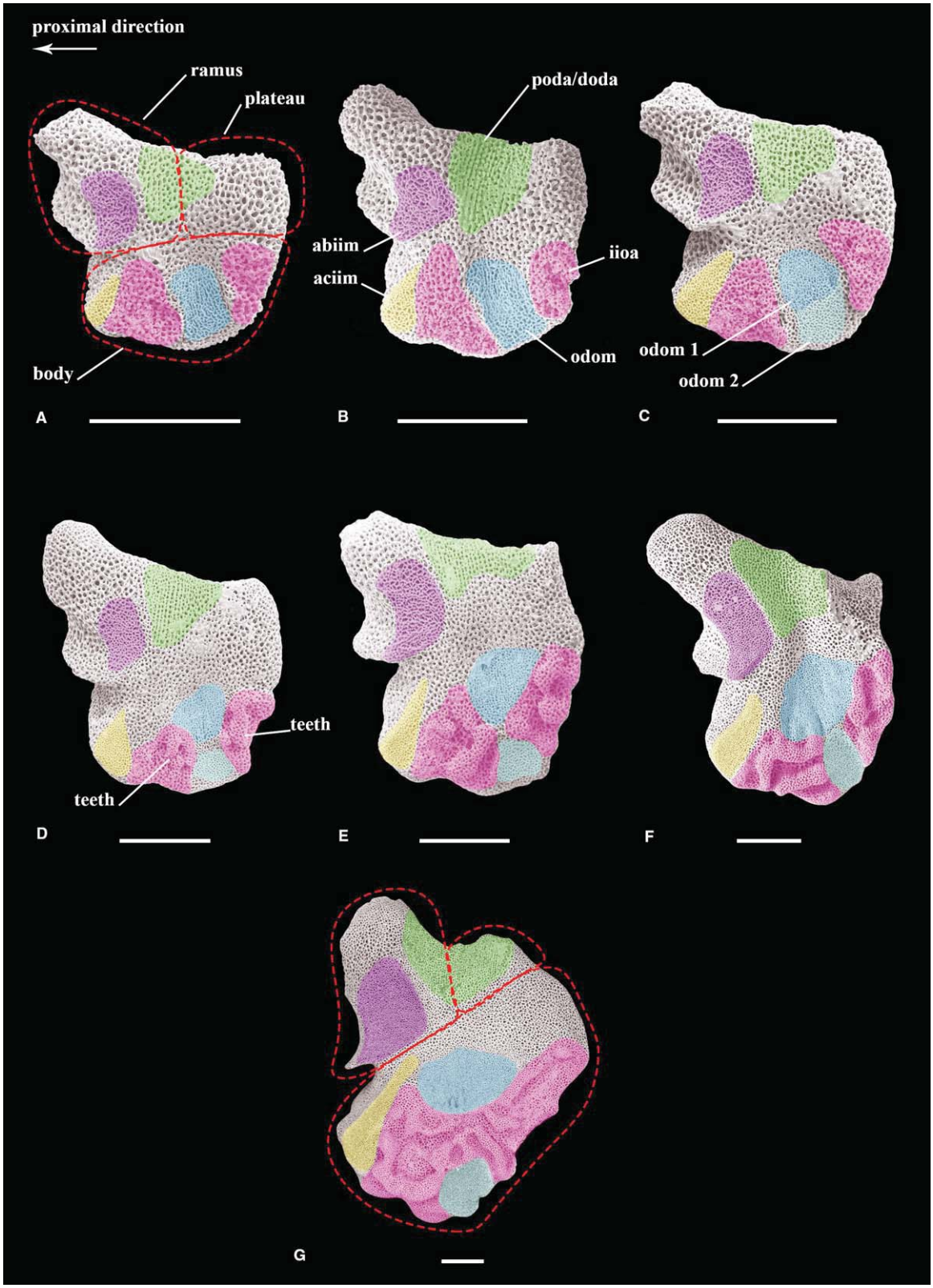

Fig. 5 Scanning electron microscopy (SEM) images of oral ossicles in interradial view. (A) Z1; (B) Z2; (C) Z3; (D) Z4; (E) Z5; (F) Z6; (G) Z7. Coloured areas indicate the presence of a differentiated stereom. In purple: insertion of the muscle *abiim*; in yellow: insertion of the muscle *aciim*; in blue: insertion of the muscle *odom* (*odom1* and *odom2*); in pink: articulation *iioa*; in green: articulation *poda* and *doda*. Actinal to the bottom. See Table 2 for abbreviations. Scale bars: 500 μm.

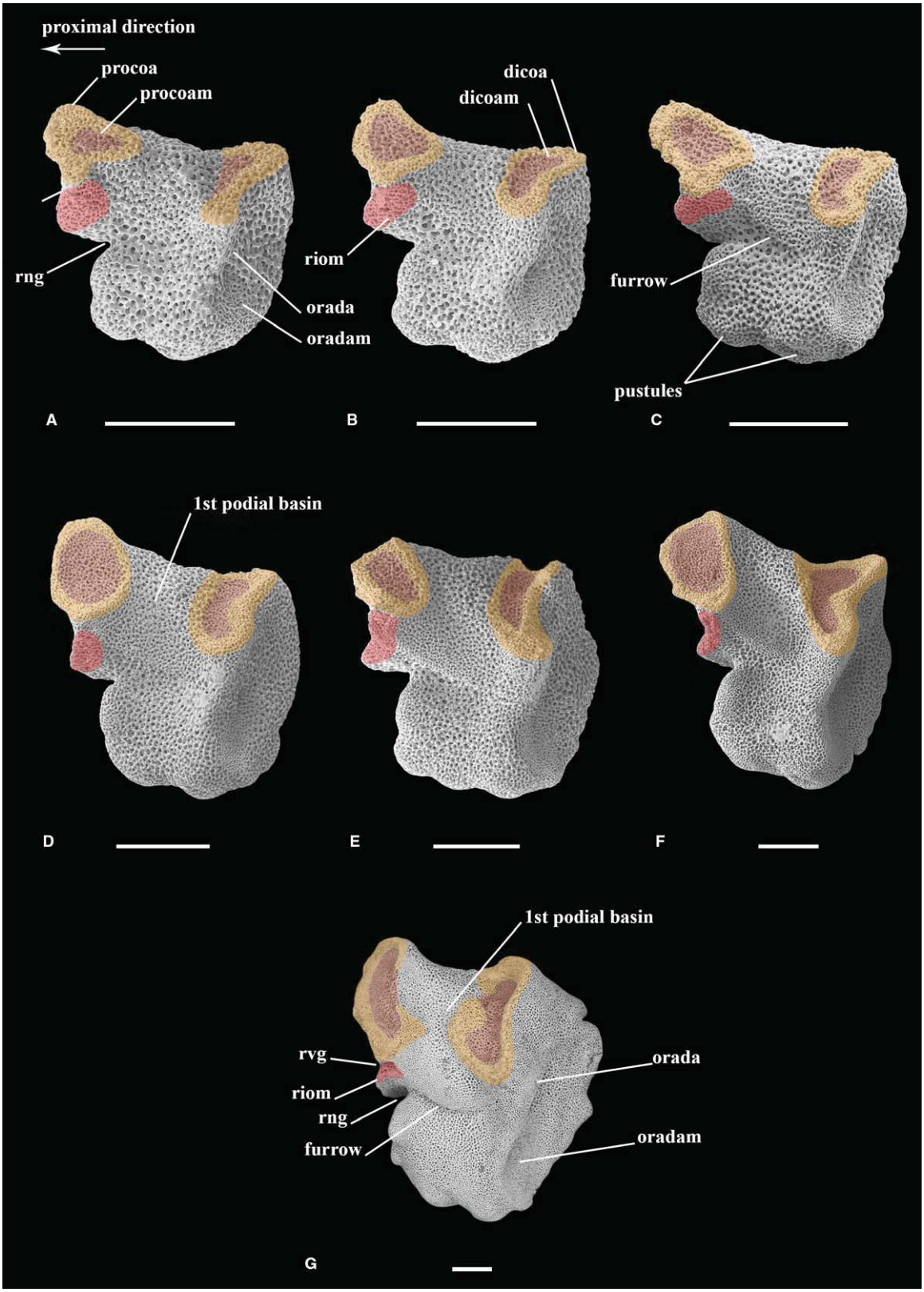

Fig. 6 Scanning electron microscopy (SEM) images of oral ossicles in radial view. (A) Z1; (B) Z2; (C) Z3; (D) Z4; (E) Z5; (F) Z6; (G) Z7. Coloured areas indicate the presence of a differentiated stereom. In red: insertion of the muscle *riom*; in brown: insertion of the muscle *procoam* and *dicoam*; in orange: articulation *procoa* and *dicoa*. Actinal to the bottom. Scale bars: 500 μm.

of Z4 and Z5, and develop further in Z6 and Z7 (Fig. 7G,K). In specimens Z1, Z2, Z3 and Z4 the complex *dicoa/dicoam* possess *wings* and the abactinal side is longer than the actinal side. The complex *dicoa/dicoam* is therefore organized similarly to the base of the ambulacrals (Fig. 7A–D). However, the *wings* are reduced on Z4, and completely absent in Z6 and Z7 (Fig. 7E–G,I,K,L).

The head of the ossicle grows faster than the distal process (Fig. 7A–K; Fig. S1; Table S1 in SOM). In Z1, the head represents one-third of the height of the ossicle (proximal height = 342 μm, distal height = 910 μm; Table S1 in SOM 1), whereas in Z7 the head represents more than half of the total height (proximal height = 2160 μm, distal height = 4006 μm; Table S1 in SOM 1). In addition, the height of the ossicles (both proximal and distal) increases faster than the length of the ossicles. The distal height of Z7 is 3.7 times the distal height of Z1, while the length of Z7 is 4.4 times the length of Z1 (length of Z1 = 650 μm, length of Z7 = 2432 μm; Fig. 7A–K; Fig. S1; Table S1 in SOM). Thus, the stretching of the ambulacral head during growth is responsible for the drastic change of ossicle shape.

Odontophore

The odontophore gets wider during growth, from a squarish shape in Z1 and Z2 to being clearly wider than long in Z5–Z7 (Fig. 8). The articulations *poda* and *doda* are fused in all of the imaged specimens, suggesting that the feature is present since the formation of the oral frame, and not acquired during growth (Fig. 8A–G). The actinal side is composed of the *odom* at the centre, surrounded by the fused articulations *poda/doda* (Fig. 8A–G). The articulation is made of galleried stereom in all specimens. In Z1, Z2, Z3 and Z4 the *odom* is made of fine labyrinthic stereom (Fig. 8A–D). It is completely replaced by retiform stereom in Z6 and Z7 (Fig. 8F,G), Z5 presenting an intermediate state with both labyrinthic and retiform stereom (Fig. 8E). The abactinal side is composed of flat, undifferentiated stereom (Fig. 8H–L). Four of the odontophores of specimen Z7 were imaged, and all of them present an abactinal *bump* (Fig. 8L). The *bumps* have a concave extremity, and are connected to an inner wall composed of soft tissue and actinals (Fig. 9). However, the stereom at the top of the *bump* is undifferentiated, presenting no sign of articulation or muscle insertion.

Ambulacrals

A total of 126 ambulacrals were sorted according to their size to represent the variation of shape and size along the arm from proximal to distal ambulacrals of each specimen. They were then imaged, of which 36 were imaged and measured in actinal view. Three measurements were taken: the height, from the top of *teeth* to the actinal point of the *base*; the length of the head taken at the base of the *teeth*; and the shortest length of the central constriction under the *actam* (Figs 10H and 11; Table S2 in SOM).

The general shape of the ossicle evolves and new features differentiate with growth (Fig. 10). The smallest ambulacrals ($h < 528$ μm) show a simple hourglass shape, with a long head and two *wings* at its *base*. They are entirely composed of undifferentiated labyrinthic stereom (Fig. 10A,B). The muscles insertions (*abtam*, *actam*, *padam* and *dadam*) and the articulations on the *base* (*pada*, *dada*) are visible on ambulacrals larger than 760 μm (Fig. 10C). The smallest observed ambulacral with *teeth* measures 783 μm in height and belongs to specimen Z1. Thus, *teeth* are present on the biggest ambulacrals of all studied specimens. As on the oral and the first ambulacrals, a *furrow* is situated on the actinal side of the ambulacrals, under the *actam*. The *furrow* is absent on the most proximal ambulacrals of specimens Z1, Z2 and Z3. The smallest observed ambulacral with a *furrow* measures 1198 μm in height and belongs to the specimen Z4.

During ontogeny, the hourglass shape of the youngest ambulacrals progressively disappears (Fig. 10A–H,K,M,P). The ambulacral height increases approximately twice as fast as *teeth* length and centrum length, resulting in a more elongated ossicle (Fig. 10). The *shaft* of the ossicle grows faster than the head and the *base* (Fig. 11; Table S2 in SOM), which contributes to a flattening of the shape of the largest ossicles (Fig. 10E–H,M,P). The *wings* progressively disappear on the most proximal ambulacrals of the largest specimens (Fig. 10O–Q).

Zoroasteridae are special among the Forcipulatacea, notably because of their deeply sunken mouth and their adoral carina composed of many adambulacrals. Both of these characters have an impact on the morphology of the adambulacrals as well as the ambulacrals. The ambulacrals of the adoral carina are more compressed, with a head larger than the *base*, and a bent abactinal axis, whereas ambulacrals of the arms tend to be straight (Fig. 10O–Q). No superambulacrals were observed in most specimens, except for Z7, in which few, small superambulacrals are present.

Adambulacrals

All the articulations and muscles connecting the adambulacrals to the ambulacrals (i.e. *padam*, *dadam*, *pada*, *dada*) are distinguishable on the stereom of the ossicles of specimen Z1 (Fig. 12A,B), with similar arrangements in the bigger and older adambulacrals. In specimens Z1, Z2, Z3 and Z4, the *dada* occupies a unique area (Fig. 12A), whereas it is well separated into two areas, with a notch on the adradial area, in the adambulacrals of Z6 and Z7, even in the smallest ones (Fig. 12D,G,I,J). In specimen Z5, some adambulacrals show a transition state, with a still unified *dada*, but showing two different parts separated by a narrow band of irregular, perforate stereom. The muscles and articulations that connect the adambulacrals

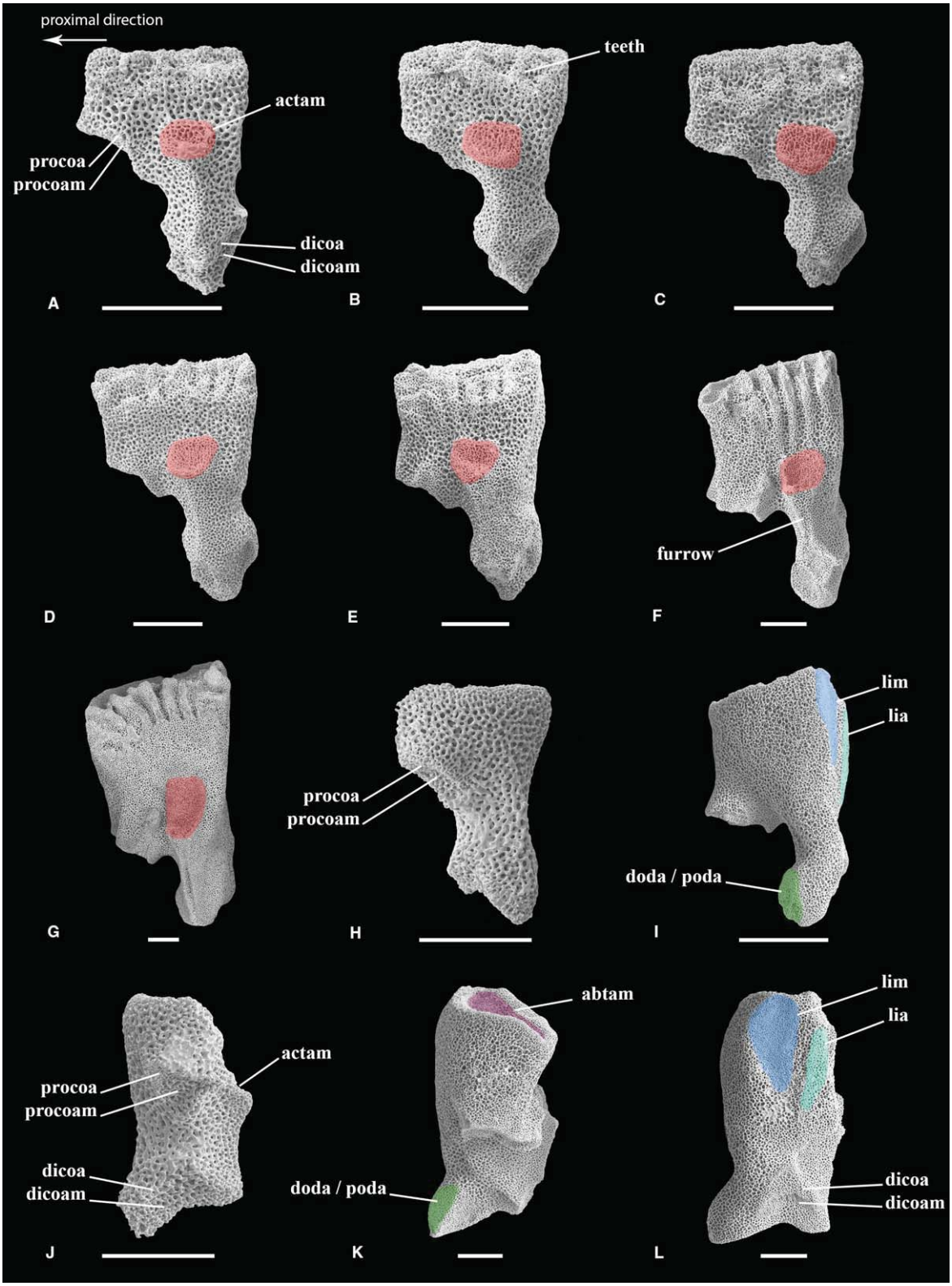

Fig. 7 Scanning electron microscopy (SEM) images of first ambulacrals, (A–G) in actinal view; (H–I) in abactinal view; (J–K) in proximal view; (L) in distal view. (A) Z1; (B) Z2; (C) Z3; (D) Z4; (E) Z5; (F) Z6; (G) Z7; (H) Z1; (I) Z6; (J) Z1; (K, L) Z6. Coloured areas indicate the presence of a differentiated stereom. In red: insertion of the muscle *actam*; in purple: insertion of the muscle *abtam*; in dark blue: insertion of the muscle *lim*; in light blue: articulation *lia*; in green: articulation poda and doda. Actinal to the bottom. See Table 2 for abbreviations. Scale bars: 500 μm.

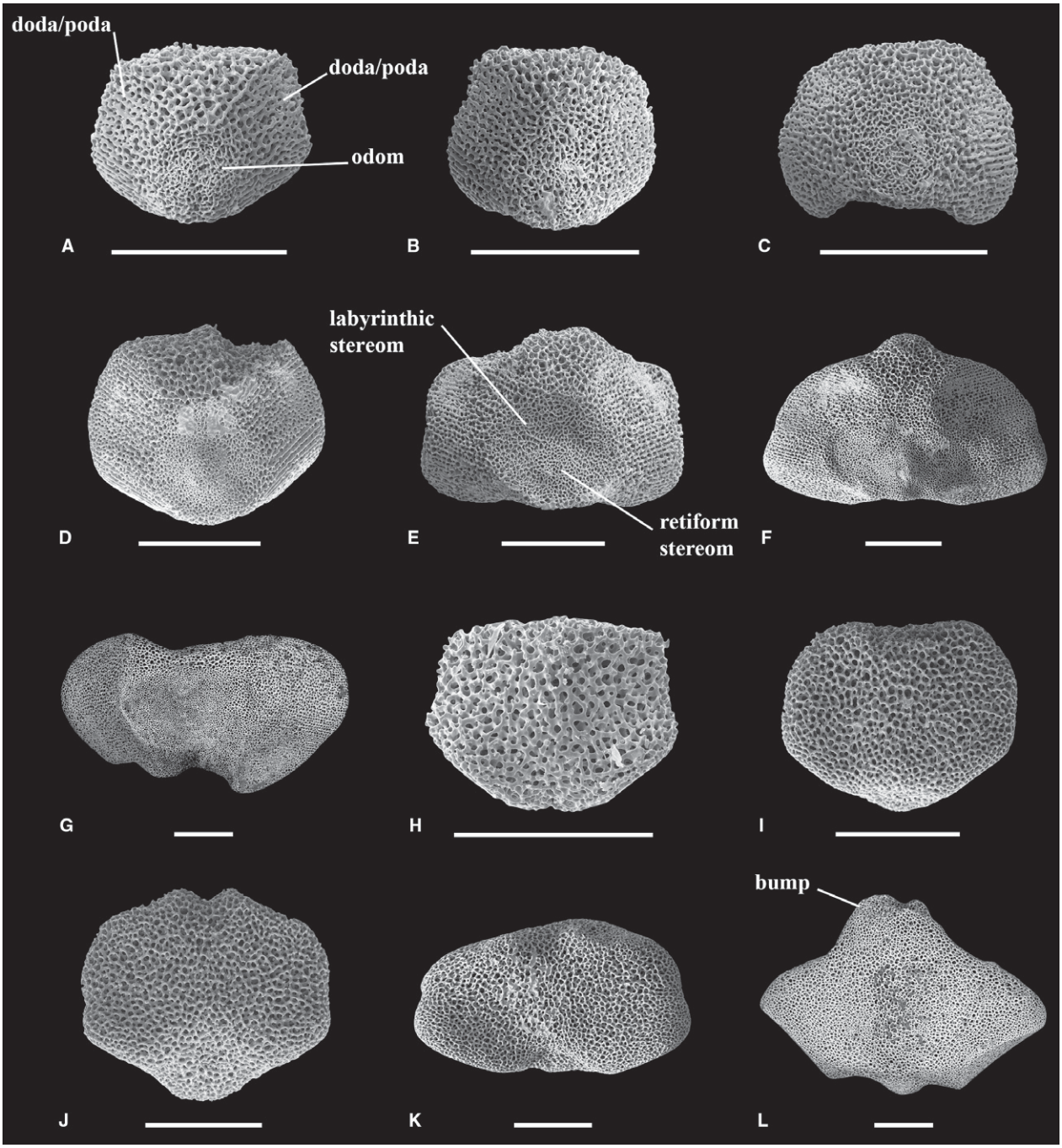

Fig. 8 Scanning electron microscopy (SEM) images of odontophores, (A–G) in actinal view; (H–L) in abactinal view. (A) Z1; (B) Z2; (C) Z3; (D) Z4; (E) Z5; (F) Z6; (G) Z7; (H) Z1; (I) Z4; (J) Z5; (K) Z6; (L) Z7. Proximal direction to the bottom. See Table 2 for abbreviations. Scale bars: 500 μm.

(interradam and interrada) are not visible on Z1 (Fig. 10A–C). The interrada becomes visible first on the proximal face of the adambulacrals of Z4, and then on both sides of the adambulacrals of Z5, Z6 and Z7 (Fig. 12D–J). The *interadam* is relatively small in Z1, Z2, Z3 and Z4 (Fig. 10A–C), and in the smallest adambulacrals of Z5, Z6 and Z7 (Fig. 12J,K), but it becomes larger in the largest adambulacrals of the series (Fig. 10D–H). All articulations on the adambulacrals are made of irregular perforate stereom.

Zoroasteridae possess a particularly long adambulacral carina involving more than three adambulacrals. Because to our knowledge no precise definition is available in the literature for the adambulacral carina, we choose to define it as

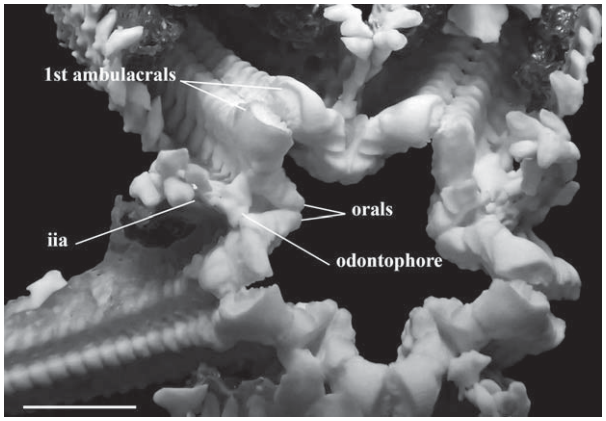

Fig. 9 Abactinal view of the oral frame of the specimen Z7, partially dissected. See Table 2 for abbreviations. Scale bar: 5 mm.

having to follow these two criteria: (i) having at least the most proximal adambulacral in contact with the most proximal adambulacral of the adjacent arm on its adradial side; and (ii) the presence of a dimorphism between the adambulacrals of the carina and the rest of the adambulacrals. In the case of *Z. fulgens*, the adambulacrals of the adoral carina are triangular, with the abactinal edge larger than the actinal edge. They also possess a few *teeth* on their adradial edge (Fig. 10F,L). The *teeth* of the adambulacrals are associated with muscles that tightly bound together the adambulacrals of the carina.

Zoroasteridae have alternatively carinate and non-carinate adambulacrals. The adambulacral carinae are adradial extensions of the plate margin (Fig. 12D–K,N). In order to determine the appearance size of the adradial extension and the evolution of the adoral carina, 24 specimens from size $R = 9$ mm to $R = 47$ mm were examined, in addition to Z1–Z7 (Table S3 in SOM). There is no contact between the first adjacent adambulacrals of the three smallest specimens ($R = 9$, 11 and 12 mm). The contact appears first at $R = 13$ mm. However, the adambulacrals of the adoral carina are not morphologically differentiated at early stages. From $R = 18$ mm to $R = 36$ mm (13 specimens studied; Table S3 in SOM), the adoral carina can be composed of one–two pairs of adambulacrals (five pairs per specimens), but they remain undifferentiated. The long adoral carina develops progressively during ontogeny. From $R = 35$ mm to $R = 66$ mm (10 specimens studied; Table S3 in SOM), the adoral carina can be composed of three–four pairs of adambulacrals. Adambulacrals of the adoral carina start to be differentiated from the other adambulacrals from specimens larger than $R = 36$ mm, by showing a more triangular shape and the appearance of *teeth* (Fig. 10F,L).

Adradial extensions start to be visible on adambulacrals from $R = 32$ mm, but not on all specimens. All specimens larger than $R = 39$ mm possess alternatively carinate and non-carinate adambulacrals (six specimens measured; Table S3 in SOM).

The number of spines per ossicle was counted on SEM images, assuming one *pustule* equals one primary spine, and one *bump* equals one secondary spine. The number of spines varies with the size of the adambulacral and the adradial extension. Adambulacrals with adradial extension usually bear more spines. Adambulacrals bear one or two spines on small juveniles, depending on their size; however, no *pustules* are visible on the smallest adambulacrals (Fig. 10A–C,M). In larger specimens (Z5, Z6 and Z7), there are between two and four spines, according to the size of the adambulacrals and the presence or absence of the adradial extension (Fig. 10N).

Pedicellariae

Straight forcipulate pedicellariae are found on the oral and adambulacral spines of even the smallest specimens studied ($R = 9$ mm). Because of preservation, the pedicellariae of adambulacral spines are rather rare in specimens smaller than $R = 24$ mm. Eight specimens out of 12 with $R < 24$ mm possess pedicellariae on the adambulacral spines (Table S3 in SOM). All specimens studied possess large duck-billed pedicellariae on the oral spines.

Discussion

How does an ossicle grow?

Asteroid ossicles commence growth as intracellular spicules that later differentiate into ossicles through the addition of extracellular calcite deposits (Ben Khadra et al. 2015a;

Fig. 10 Scanning electron microscopy (SEM) images of ambulacral ossicles in actinal view (A–H, K, M, P), distal (I, L, N, O) and proximal view (J, Q). Actinal to the bottom. The ambulacrals (A–H) are ordered from the smallest to the biggest (Table S2 in SOM). The ambulacrals (K–M) belong to the specimen Z7, and the ambulacrals (O–Q) are part of the adoral carina of the specimens Z6 and Z7. Each ambulacral is coded as follows: the number of the specimen (i.e. Z1, Z2, …, Z7), plus the number of the SEM images that was used for the measurements (i.e. from 001 to 126). See Table S2 (in SOM) for measurements. (A) Z2, photo no. 052; (B) Z2, photo no. 049; (C) Z2, photo no. 050; (D) Z1, photo no. 034; (E) Z3, photo no. 037; (F) Z4, photo no. 018; (G) Z5, photo no. 018; (H) Z6, photo no. 023; (I) Z1, photo no. 045; (J) Z1, photo no. 046; (K) Z7, photo no. 061; (L) Z7, photo no. 076; (M) Z7, photo no. 052; (N) Z6, photo no. 030; (O) Z6, photo no. 021; (P) Z7, photo no. 029; (Q) Z7, photo no. 034. Coloured areas indicate the presence of differentiated stereom. In dark red: insertion of the muscle *actam*; in purple: insertion of the muscle *abtam*; in light red: insertion of the muscle *padam*; in orange: insertion of the muscle *dadam*; in dark blue: insertion of the muscle *lim*; in light blue: articulation *lia*; in light orange: articulation *dada*; in yellow: articulation *pada*. See Table 2 for abbreviations. Scale bars: 500 μm (A–M); 1 mm (N–Q).

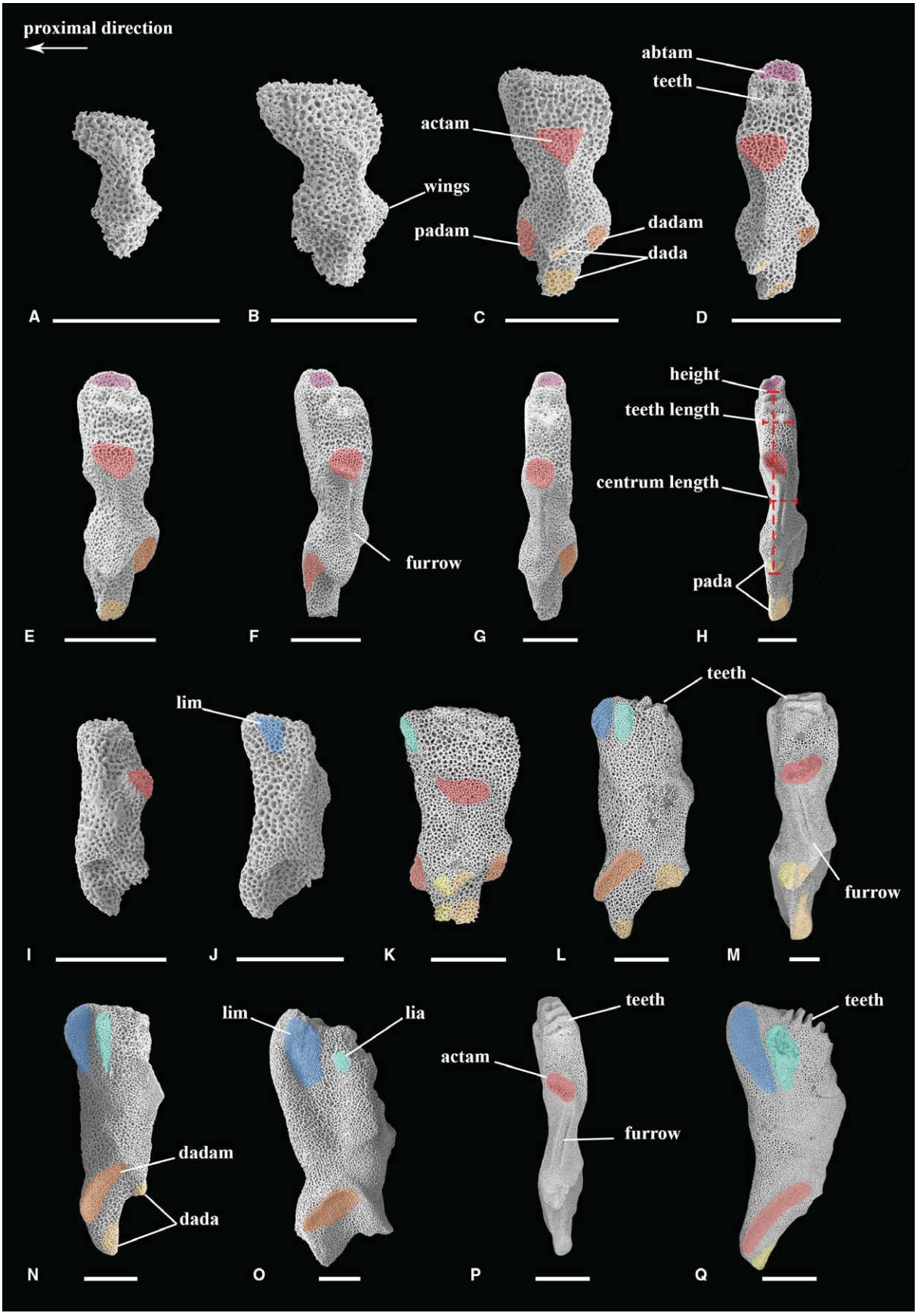

Czarkwiani et al. 2016). This mode of growth has been observed in early post-metamorphic stages (Komatsu, 1975; Komatsu et al. 1979; Komatsu & Nojima, 1985; Pernet et al. 2017), as well as during arm regeneration (Ben Khadra et al. 2015a, 2017; Czarkwiani et al. 2016) or spine regeneration (Dubois & Jangoux, 1990). It has also been observed in other echinoderms, like sea urchins (Okazaki, 1960; Chen & Lawrence, 1986), sea cucumbers (Stricker, 1985) and brittle stars (Czarkwiani et al. 2013).

Dubois & Jangoux (1990) described three different stages during the regeneration of the spines of *Asterias rubens*: (i) the first mineral deposit; (ii) growth of the ossicle; and (iii) differentiation of the stereom. The latter two stages are consistent with our observations. The first stage, which corresponds to the formation of calcified spicules, is not observable in our data set, because the spicules are removed during the bleaching process.

Here, we show that the growth of ossicles can be characterized with three parameters: (i) the size; (ii) the shape; and (iii) stereom differentiation. The size of ossicles increases during ontogeny. The shape of an individual ossicle depends both on the size of the specimen and the size of the ossicle itself. The shape of an ossicle depends not only on the size of the specimen, but also on its position in its series (e.g. ambulacral series, marginal series, etc.). For example, the smallest ambulacrals imaged for specimen Z7 (Fig. 10K: Z7061, height = 1193 μm) are proportionally longer and with a less marked centre than ambulacrals of similar size in specimens Z3 and Z4 (Fig. 10E,F: Z3037 and Z4018, respectively, height = 998 μm and 1277 μm). Thus, the shape of serial ossicles evolves during life according to its position in the series. Similar observations have been recorded for the ossicles composing the stalks of crinoids (Améziane & Roux, 2005).

Younger ossicles not only have different shapes compared with older, homologous ossicles (e.g. ambulacrals and adambulacrals; Figs 10 and 12), but they are also made of undifferentiated labyrinthic stereom and lack differentiated structures like muscle insertions, articulation areas and the presence of *teeth*. This is particularly visible on ambulacrals where the specialization of the stereom can be observed through the ontogenetic series (Fig. 10A–H). The youngest ambulacrals (Fig. 10A) are made entirely of labyrinthic stereom of homogeneous density. As size increases, different areas of specialized stereom start to appear (Fig. 10B–H): the stereom becomes thinner where muscles are inserted (i.e. *actam*, *abtam*, *padam*, *dadam*; Fig. 10), and articulation areas strengthen with irregular perforate stereom (*sensu* Smith, 1980; i.e. *dada*, *pada*, lia; Fig. 10). These structures are invisible during the early life of ossicles.

How does an asteroid grow?

Right after metamorphosis, all asteroids have a rounded to stellate body outline without developed arms (Komatsu, 1975; Komatsu et al. 1979; Komatsu & Nojima, 1985; Sumida et al. 2001; Gale, 2011; Pernet et al. 2017). The first five ossicles to appear around the body margin are the terminal ossicles and they stay at the arms' apex during the entire life of the asteroid. On the dorsal side, five interradial ossicles (also call primary interradials) appear between two adjoining terminals, and a sixth plate usually appears at the centre of the dorsal face (the central or centrodorsal). Radial ossicles (or primary radials) generally appear soon after. With increasing size and arm elongation, marginal ossicles form along the body margin between the terminals. In parallel, addition of new abactinal plates takes place at the axis of the arms (carinals and radial abactinals), as well as between the central ossicle and the interradials, and between the interradials and the marginal frame. The madreporite develops along the margin of the body and shifts progressively towards the centre of the disc with the addition of new abactinals (Komatsu, 1975; Komatsu et al. 1979; Komatsu & Nojima, 1985; Gale, 2011). The madreporite can fuse with an interradial in some taxa (Fig. S2 in SOM).

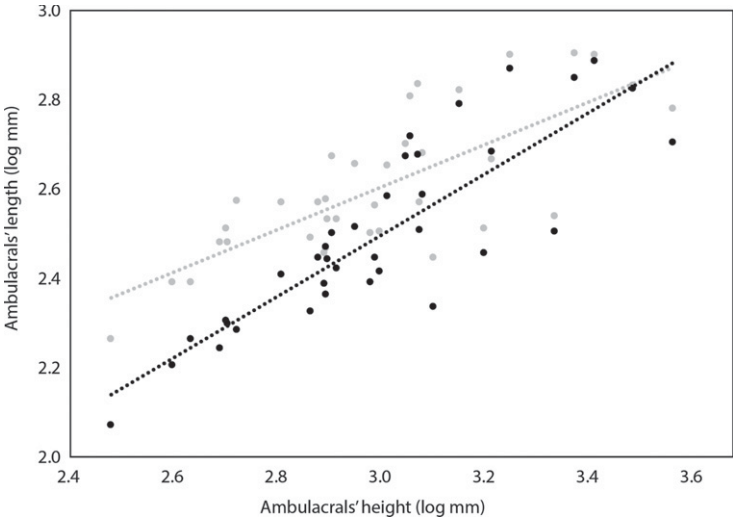

Fig. 11 Length of the ambulacral elements according to their height, all measurements have been log-transformed. In grey: the *teeth* length, $y = 0.472x + 1.184$, $R^2 = 0.567$. In black: the centrum length, $y = 0.681x + 0.451$, $R^2 = 0.73$.

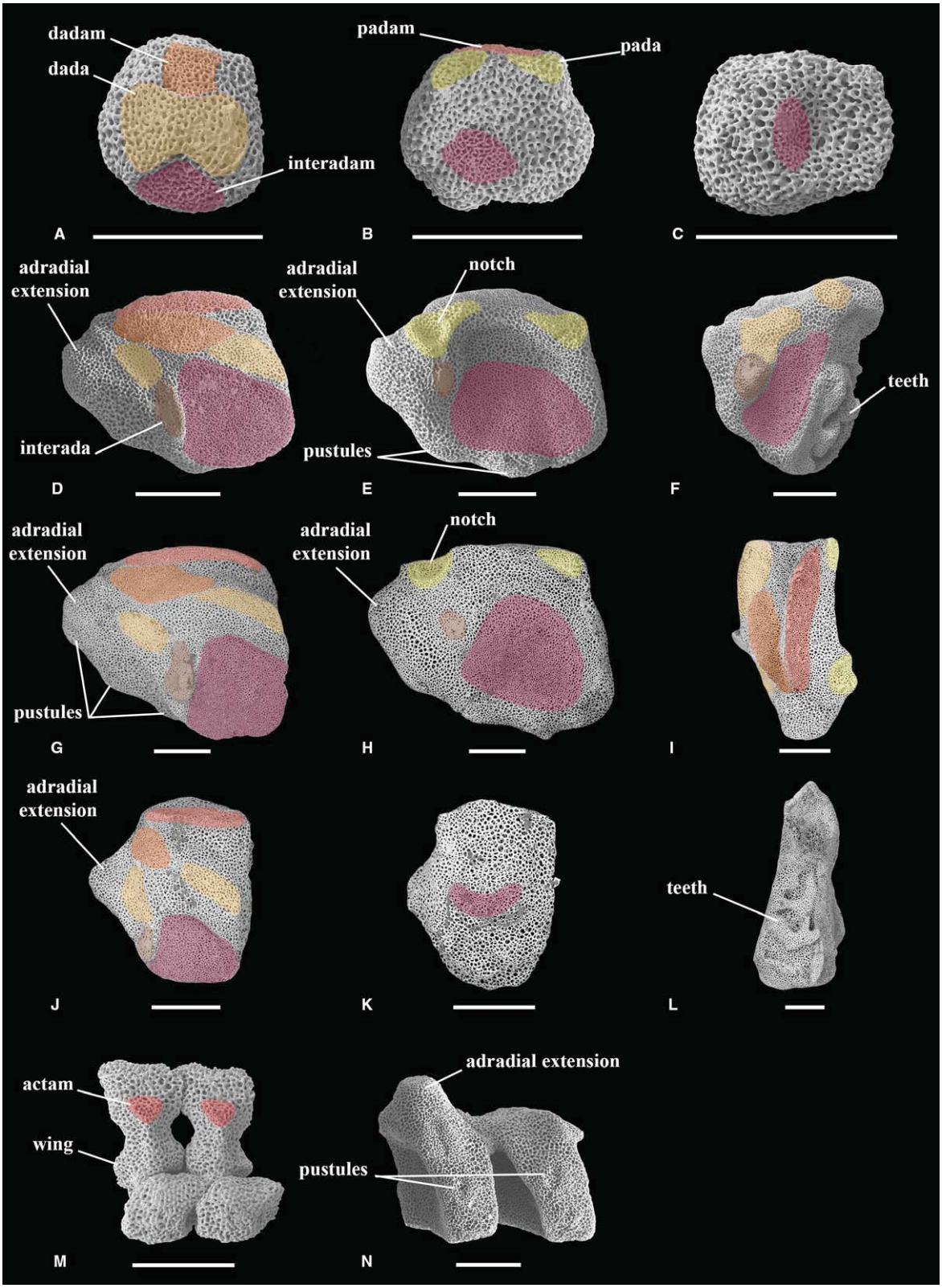

Fig. 12 Scanning electron microscopy (SEM) images of the adambulacrals in proximal (A, D, F, G, J), distal (B, E, H), actinal (C, K, M, N), abactinal view (I) and interradial view (L). (A–C) Z1; (D–F) Z6; (G–L) Z7; (M) Z1; (N) Z6. Coloured areas indicate the presence of a differentiated stereom. In purple: insertion of the muscle *interadam*; in light red: insertion of the muscle *padam*; in orange: insertion of the muscle *dadam*; in brown: articulation *interada*; in light orange: articulation *dada*; in yellow: articulation *pada*. Actinal to the bottom. See Table 2 for abbreviations. Scale bars: 500 μm.

The extraxial-axial theory (EAT) was developed based on empirical data to recognize homologies between the different clades of echinoderms, by separating the skeleton into two parts according to their growth dynamics: axial and extraxial (Mooi et al. 1994). According to Mooi & David (2000), axial skeletal elements are added following the ocular plate rule (OPR), which means that new axial elements are added at the distal end of ambulacrals series, typically associated with the terminal plate. For asteroids, this means that new ambulacrals and adambulacrals are formed right under the terminal plate, proximally to the terminal podia (Mooi & David, 2000, 2008). On the other hand, extraxial elements are thought to form anywhere, but sometimes show secondary organization. Thus, the EAT and the OPR provide a guideline on how asteroids grow.

1 Ossicles of the axial skeleton (ambulacrals and adambulacrals) are added progressively below the terminal plate. The earliest formed (older) ossicles are found close to the mouth, and the last formed (younger) ones towards the tips of the arms. Orals and first ambulacrals are the most proximal elements belonging to the axial skeleton.
2 Ossicles of the perforated extraxial skeleton (actinals, abactinals and odontophores) can be organized serially but their growth pattern may not necessarily follow the OPR. The newly added plates fill open space in the skeletal framework during growth (e.g. actinal ossicles are added between the adambulacrals and the marginals).
3 Marginals and carinals belong to the extraxial skeleton but, in some taxa, their growth pattern follows that of the axial skeleton in that new ossicles are added along the proximal side of the terminal. Marginal and carinal rows, however, can be interrupted during growth in some taxa or be disrupted by insertion of elements of the perforated extraxial skeleton.

Our observations on *Z. fulgens* are in accordance with the three statements phrased above, as we observe that the youngest ambulacrals and adambulacrals are formed behind the terminal tube foot under the terminal ossicle (Fig. 3M), and that both actinals and abactinals fill gaps between the adambulacrals and the marginals and the marginals and the carinals, respectively (Fig. 3M). It is remarkable that marginals and carinals seem to follow the OPR (Fig. 3L,M). The carinals originate inside the notch of the terminal plate, which is especially deep in small juveniles. The youngest carinal is therefore in a more distal position than the youngest marginal. Up to four carinals can fit in the notch of the terminal ossicle (Fig. 3L).

Recent work on the regeneration process in echinoderms, especially the regeneration of the asteroids and ophiuroids arms, has shown that regeneration follows a 'distalization-intercalation' model (Ben Khadra et al. 2015a,b, 2017; Czarkwiani et al. 2016). The regeneration can be divided into three main phases: (i) the repair phase during the first hours/days post-amputation; (ii) the early regenerative phase; and (iii) the advanced regenerative phase (Candia Carnevali & Bonasoro, 2001; Ben Khadra et al. 2015a,b, 2017). It is during the early regenerative phase that 'distalization-intercalation' occurs, i.e. the most distal structures (i.e. the terminal ossicle and the terminal podia for asterozoans) are the first to regenerate and they will eventually drive the rest of the regeneration process. The other ossicles are created inside the axial gap formed between the stump and the regenerating bud (Candia Carnevali & Bonasoro, 2001; Ben Khadra et al. 2015a,b, 2017; Czarkwiani et al. 2016). The distalization-intercalation process of regeneration may reflect the natural way asteroids grow, and is in accordance with the EAT and the OPR. Indeed, the terminal ossicles and the ossicles of the disc are the first ones to appear right after metamorphosis (Fig. 1; Fewkes, 1888; Gemmill, 1912, 1914, 1920; Komatsu, 1975; Komatsu et al. 1979; Siddall, 1979; Komatsu & Nojima, 1985; Sumida et al. 2001; Lopes & Ventura, 2016). Thereafter, asteroid juveniles grow by adding new ossicles at the tip of their arms, proximally or below the terminal ossicle (Fig. 3L,M; Fewkes, 1888; Gemmill, 1912, 1914, 1920; Komatsu, 1975; Oguro et al. 1976; Komatsu et al. 1979; Siddall, 1979; Komatsu & Nojima, 1985; Mooi & David, 2000; Sumida et al. 2001; Lopes & Ventura, 2016). The regeneration process of a lost arm is very similar to early ontogeny.

Czarkwiani et al. (2016) showed that during the early and late regenerative phase of *Amphuira filiformis* (Ophiuroidea), the lateral spicules (i.e. future lateral arm plates) appear before the vertebral spicules (i.e. future vertebrae; Fig. 4). This is particularly important, because the vertebrae are interpreted as axial elements, homologous to the ambulacrals of asteroids (Mooi & David, 2000). This challenges the EAT because: (i) the vertebral spicules are formed between podial bulges but far away from the terminal ossicle, and therefore away from the structure that is supposed to drive the creation of axial elements; and (ii) because the lateral spicules are formed before the vertebral spicules, in a more distal position, which is not expected by the EAT. But this example shows perfectly the need for future studies on the growth and regeneration of asteroids. Ben Khadra et al. (2015a,b, 2017) have provided new insight into asteroid regeneration, but the process of generation and regeneration of the ossicle is yet to be studied in more detail.

Ontogeny and recognition of homologies

Zoroaster fulgens is the only species of the genus *Zoroaster* currently recognized in the North Atlantic. Several species of *Zoroaster* had initially been described from this region (*Z. ackleyi* Perrier, 1881; *Z. diomedae* Verrill, 1884; *Z. longicauda* Perrier, 1885; *Proganaster grimaldii* Perrier, 1891; *Z. trispinosus* Koehler, 1896), but these were all synonymized with *Z. fulgens* by Downey (1970), as confirmed by Clark &

Downey (1992). Downey (1970: 15) argued that the 'Presence, absence or degree of development of the superomarginal spines, and the relative width of the carinal plates are the sole characters on which the Atlantic *Zoroaster* have been separated. These characters, are vague and unsatisfactory to begin with, [and] prove extremely variable throughout the range of the genus [...]'. More recently, however, Howell et al. (2004) argued that there are three morphotypes of *Z. fulgens* in the Porcupine Seabight distributed by depth ranges: a robust form (925–1750 m); a slender form (1300–2200 m); and a long-armed form (3330–4020 m). They argued that the morphotypes are likely to be reproductively isolated, and thus to represent three different species. They concluded by advocating for a taxonomic revision of the genus using both molecular and morphological data. This study may prove useful in disentangling this problem, as we here provided a comparative basis by describing the slender morphotype in detail.

Our comparative study reveals that the overall anatomy of the Zoroasteridae is quite singular and stands out when compared with other forcipulatacean asteroids. However, juvenile *Z. fulgens* share more similarities with other Forcipulatacean than the adult (Z7), especially in the morphology on the orals and first ambulacrals (Figs 5–7). Orals of the juveniles (Z1–Z6) are similar in shape to orals in *P. ochraceus* (Asteriidae) and *N. forcipatus* (Stichasteridae; Fig. S2C,E in SOM). They all possess a *ramus* and a well-defined *body*, separated by the *plateau* that forms a flat to obtuse angle with the *ramus*. However, orals of *Z. fulgens* differ by: (i) their unique articulation with the odontophore (*poda* and *doda* are fused; Fig. 5) where both the *poda* and *doda* are distinct on *P. ochraceus* and *N. forcipatus*; and (ii) the presence of large *iioa* compared with the *iioa* of *P. ochraceus* and *N. forcipatus* (Fig. 5; Fig. S2C,E in SOM). The heads of the first ambulacrals are small in Z1, Z2 and Z3 (Fig. 5A–C), as are those of other Forcipulatacea (Fig. S2F–H in SOM), whereas the first ambulacral's head of Z4, Z5 and especially Z6 and Z7 are taller and larger than usually found in the Forcipulatacea (Fig. S2F–H in SOM). This reveals allometric scaling during the ontogeny of *Z. fulgens*. There is a need to describe and quantify the ontogeny of more asteroid species, especially of the ossicles, in order to build a comprehensive framework to understand skeletal growth and the differentiation of morphological features.

A large number of characters appear progressively during ontogeny. Studying adult specimens is therefore essential to avoid missing important key characters, but because of the serial nature of some ossicles (e.g. ambulacrals, adambulacrals, marginals) the relative size and position of the ossicles along the arm are also crucial. Because serial ossicles are created continuously during the life of each individual, each ossicle possesses a unique history. The smallest ambulacrals found in the adult (Z7) do not look the same as the smallest ambulacrals found in juveniles. Améziane & Roux (2005) made similar observations on the crinoid *Guillecrinus*. They observed phenotypic plasticity in the ossicles forming the stalk, from the first ossicles possessing bilateral articulations to pentaradiate symmetry appearing later in life in *Guillecrinus*. They concluded that there is a close relation between the phenotype of the ossicles and the hydrodynamic conditions during the life of the individual. Here we show that the shape of the smallest ambulacrals and adambulacrals of Z7 does not match the shape of the ones found in Z1, Z2, Z3, Z4 or Z5. Each ossicle possess its own history and its own ontogeny. Therefore, the complete series of ossicles found in an adult specimen does not allow necessarily an interpretation of its earlier ontogenetic stages. Further investigations need to be done to evaluate how much the phenotype evolves during the life of the specimen. Consequently, particular attention must be given to serial ossicles, especially when they are utilized for phylogenetic inferences in order to avoid non-homologous comparison.

The monophyly of the Post-Palaeozoic Asteroidea is now widely accepted by the scientific community; however, the relationships of the main orders (Velatida, Valvatacea, including Paxillosida, Forcipulatacea, Spinulosida) are still strongly debated using morphological and molecular data (Blake, 1987; Gale, 1987a, 2011; Janies et al. 2011; Mah & Foltz, 2011a,b; Mah & Blake, 2012; Feuda & Smith, 2015; Linchangco et al. 2017). The family Zoroasteridae is commonly interpreted as the sister-group to all other Forcipulatacea, their anatomy is therefore of great importance for the understanding of asteroid phylogeny (Mah, 2000, 2007; Blake & Elliott, 2003; Gale, 2011; Mah & Foltz, 2011a).

Mah (2007) performed a phylogenetic analysis of the family Zoroasteridae. He defined 70 characters, of which only 12 describe internal structures. Later, Gale (2011) published a list of 128 characters, most of them based on the oral frame (43 characters), and on ambulacrals and adambulacrals (32 characters). Our results on *Zoroaster* ontogeny suggest that more phylogenetic characters can be derived from the anatomy of the ossicles, and especially from the ossicles forming the wall skeleton (i.e. actinals, marginals, abactinals and carinals), but that more investigations of ontogenetic pathways are required for a safe approach of character definition.

Historically, Zoroasteridae are well characterized by several morphological characters: (i) a deeply sunken actinostome linked to an extensive adoral carina; (ii) the presence of four rows of tube feet proximally, often reduced to two rows distally; (iii) alternatively carinate and noncarinate adambulacrals; (iv) superambulacrals present; (v) presence of only one row of marginals; and (vi) large duck-billed pedicellariae present on adambulacral spines (but crossed forcipulate pedicellariae absent; Downey, 1970; Blake, 1987; Clark & Downey, 1992; Blake & Elliott, 2003; Mah, 2007; Gale, 2011). In our sample of *Z. fulgens*, none of the diagnostic characters is present in juveniles, with the exception of characters (v) and (vi). Characters (i), (ii) and (iii) appear sequentially during ontogeny and cannot be seen in

specimens smaller than Z5 ($R = 36$ mm). None of the juveniles possess superambulacrals (iv), and only a few small superambulacrals was observed in Z7, suggesting that the superambulacrals appear late during ontogeny, and/or are rare in this population of *Z. fulgens* from the Rockall Basin.

The number of marginal rows in the Zoroasteridae is still debated in the literature, with authors either describing only one row (Blake, 1987; Blake & Elliott, 2003; Mah, 2007; Mah & Blake, 2012; Blake & Mah, 2014) or two rows (Fisher, 1928; Downey, 1970; Gale, 2011). Blake (1978, 1987), Blake & Elliott (2003), and Blake & Hagdorn (2003) discussed criteria for recognition of the marginal series. To be interpretated as marginals, the series must arise immediately from the terminal, be morphologically differentiated from the other series (i.e. from the carinals, abactinals and actinals), and should be in a marginal position on the body. Our results clearly show that only one row of ossicles (in addition to the carinals) arises next to the terminal (Figs 3LM and 4), and is morphologially differentiated. In the literature, when only one row of marginals is recognized, it is interpreted as being inferomarginals (Blake & Elliott, 2003; Blake & Hagdorn, 2003; Mah, 2007; Mah & Blake, 2012; Blake & Mah, 2014; Villier et al. 2018). Gale (2011) introduced the forcipulatid plating rule (FPR), which describes the fairly consistent plating arrangement of the Forcipulatida. The absence of a second row of marginals in Zoroasterids is not incompatible with the FPR. Regardless of how we interpret the marginal row as superomarginals or inferomarginals, they follow the FPR because the marginals overlap both the abactinals and the actinals.

Sumida et al. (2001) mentioned the appearance of duckbilled pedicellariae on the adambulacral spines of *Z. fulgens* for specimens larger than $R = 26$ mm. Pedicellariae appear much earlier in the population from the Rockall Basin (at $R = 9$ mm), but the timing may vary from one individual to another in a single population.

Based on our observations and the comparison with other forcipulatacean asteroids (Fig. S2 in SOM), we can define six additional characters for *Z. fulgens*, based only on isolated ossicles. These characters may be useful in recognizing isolated ossicles in the fossil record, but also for further phylogenetic investigations. Characters (vii) and (viii) are assumed to be present as soon as the ossicles are formed. The other characters appear progressively during the ontogeny (visible from Z5, $R = 36$ mm). (vii) On the odontophore, the articulations *poda* and *doda* are fused. (viii) The madreporite is not completely isolated but embedded in a special cavity of the corresponding interradial. The madreporite of other forcipulatacean asteroids are generally fused with one of the primary interradials (see *P. ochraceus* and *N. forcipatus*; Fig. S2A,B in SOM). (ix) The adambulacrals of the adoral carina possess *teeth* on their adradial side. (x) The head of the first ambulacral is proportionally longer than the head of other Forcipulatacea (Fig. S2F–H in SOM). (xi) On the orals, the muscle insertion *odom* is split into two parts during the growth of the articulation *iioa*. The actinal part is reduced in adult specimens. The *odom1* is made of fine labyrinthic stereom, whereas the *odom2* is made of fine retiform stereom. Because of its position on the orals, the *odom2* cannot be connected to any part of the odontophores. Instead, we assume this muscle to connect the orals, the same way as the *aciim* and *abiim*. (xii) On the orals, the *teeth* of the *iioa* are not homologous to the *teeth* of the Brisingida. Firstly, because the stereom of the *teeth* of *Z. fulgens* is made of galleried stereom (*sensu* Smith, 1980) whereas the *teeth* of the Brisingida are made of imperforate stereom (*sensu* Smith, 1980), and secondly because the relative position of the *odom*, the *aciim* and the *iioa* (see *B. robillardi*; Fig. S2D in SOM). In the Brisingida, the *iioa* is abactinal to the *aciim*, whereas in *Z. fulgens*, the *iioa* is actinal to the *aciim*. In addition, this study shows that while the *iioa* is growing, it separates the *odom* in two different parts, whereas there is no evidence of a similar pattern in the Brisingida. The appearance of *teeth* on the *iioa* is therefore a convergence between *Z. fulgens* and the Brisingida, likely due to the fact that these two groups develop a rigid and strongly connected oral frame.

Conclusion

This is the first time, to our knowledge, that the post-metamorphic ontogeny of the ossicle of *Z. fulgens* is described. The ontogenetic series reveals that most of the historical characters used to define Zoroasteridae actually appear progressively during ontogeny, and are not visible in smaller specimens. Many new characters are described for the first time (e.g. the *teeth* on adambulacrals of the adoral carina). We furthermore show that some structures, such as the muscles insertions and articulation areas of the oral frame, can be misinterpreted, without a solid knowledge of ontogeny. Thus, there is a need for further investigation of the skeletal anatomy of more species of asteroids, but also of a study of their ontogeny, as it can help to elucidate the homology of various structures.

Acknowledgements

The authors are thankful to Marc Eleaume (MNHN) and Eric Lazo-Wasem (YPM) for the loan of the materials used in this study. The authors also thank Cyndie Dupoux (MNHN), Anouchka Sato (MNHN) and Pierre Lozouet (MNHN), as well as Lourdes Rojas (YPM) for their assistance in the management of the borrowed specimens. The authors are grateful to Christopher Mah (National Museum of Natural History) and Andy Gale (University of Portsmouth) for insightful review of the manuscript and discussion about the taxonomy of asteroids. Walter Joyce (University of Fribourg) is thanked for support during the course of this study and for reading an earlier draft of this manuscript. Christoph Neururer (University of Fribourg) is thanked for his assistance with SEM imaging. This work was supported by the Department of Geosciences of the University of Fribourg.

Author contributions

MF, LV: conception of the study. MF: data acquisition, data analysis, interpretation, draft of the manuscript. LV: interpretation, draft of the manuscript. All authors reviewed the manuscript and approved it for publication.

References

Ameye L, De Becker G, Killian C, et al. (2001) Proteins and saccharides of the sea urchin organic matrix of mineralization: characterization and localization in the spine skeleton. *J Struct Biol* **134**, 56–66.

Améziane N, Roux M (2005) Environmental control versus phylogenic fingerprint in ontogeny: the example of the development of the stalk in the genus *Guillecrinus* (stalked crinoids, Echinodermata). *J Nat Hist* **39**, 2815–2860.

Ben Khadra Y, Ferrario C, Benedetto CD, et al. (2015a) Regrowth, morphogenesis, and differentiation during starfish arm regeneration. *Wound Repair Regen* **23**, 623–634.

Ben Khadra Y, Ferrario C, Benedetto CD, et al. (2015b) Wound repair during arm regeneration in the red starfish *Echinaster sepositus*. *Wound Repair Regen* **23**, 611–622.

Ben Khadra Y, Sugni M, Ferrario C, et al. (2017) An integrated view of asteroid regeneration: tissues, cells and molecules. *Cell Tissue Res* **370**, 13–28.

Blake DB (1972) Sea star *Platasterias*: ossicle morphology and taxonomic position. *Science* **176**, 306–307.

Blake DB (1973) Ossicle morphology of some recent asteroids and description of some West American fossil asteroids. *Univ Calif Publ Geol Sci* **104**, 1–59.

Blake DB (1976) Sea stars ossicle morphology: taxonomic implications. *Thalassia Jugosl* **12**, 21–29.

Blake DB (1978) The taxonomic position of the modern sea star *Cistina* Gray, 1840. *Proc Biol Soc Wash* **91**, 234–241.

Blake DB (1987) A classification and phylogeny of post-Palaeozoic sea stars (Asteroidea: Echinodermata). *J Nat Hist* **21**, 481–528.

Blake DB, Elliott DR (2003) Ossicular homologies, systematics, and phylogenetic implications of certain north american carboniferous asteroids (echinodermata). *J Paleontol* **77**, 476–489.

Blake DB, Hagdorn H (2003) The Asteroidea (Echinodermata) of the Muschelkalk (Middle Triassic of Germany). *Paläont Z* **77**, 23–58.

Blake DB, Mah CL (2014) Comments on "The phylogeny of post-Palaeozoic Asteroidea (Neoasteroidea, Echinodermata)" by AS Gale and perspectives on the systematics of the Asteroidea. *Zootaxa* **3779**, 177–194.

Blowes LM, Egertová M, Liu Y, et al. (2017) Body wall structure in the starfish Asterias rubens. *J Anat* **231**, 325–341.

Brandt JF (1835) *Prodromus Descriptionis Animalium ab H*, pp. 203–275. Petropooli: Mertensio in orbis terrarum circumnavigatione observatorum.

Breton G (1992) Les Goniasteridae (Asteroidea, Echinodermata) jurassiques et crétacés de France : taphonomie, systématique, paléobiogéographie, évolution. *Bull Trimestriel Soc Géol Normandie Amis Mus Havre* **78**, 1–590.

Breton G (1995) La forme du corps de *Crateraster debrisi* Breton, 1992 (Asteroidea, Goniasteridae). *Bull Trimestriel Soc Géol Normandie Amis Mus Havre* **82**, 51–53.

Candia Carnevali MD, Bonasoro F (2001) Microscopic overview of crinoid regeneration. *Microsc Res Tech* **55**, 403–426.

Chen C-P, Lawrence JM (1986) The ultrastructure of the plumula of the tooth of *Lytechinus variegatus* (Echinodermata: Echinoidea). *Acta Zool* **67**, 33–41.

Clark AM, Downey ME (1992) *Starfishes of the Atlantic*. London, UK: Chapman & Hall.

Cuénot L (1887) *Contribution à l'étude anatomique des astérides*. Oudin.

Czarkwiani A, Dylus DV, Oliveri P (2013) Expression of skeletogenic genes during arm regeneration in the brittle star *Amphiura filiformis*. *Gene Expr Patterns* **13**, 464–472.

Czarkwiani A, Ferrario C, Dylus DV, et al. (2016) Skeletal regeneration in the brittle star *Amphiura filiformis*. *Front Zool* **13**, 18.

Downey ME (1970) Zorocallida, new order, and *Doraster constellatus,* new genus and species, with notes on the Zoroasteridae (Echinodermata; Asteroidea). *Smithson Contr Zool* **64**, 1–18.

Dubois P, Chen CP (1989) Calcification in echinoderms. *Echinoderm Stud* **3**, 109–178.

Dubois P, Jangoux M (1990) Stereom morphogenesis and differentiation during regeneration of adambulacral spines of *Asterias rubens* (Echinodermata, Asteroida). *Zoomorphology* **109**, 263–272.

Feuda R, Smith AB (2015) Phylogenetic signal dissection identifies the root of starfishes. *PLoS ONE* **10**, e0123331.

Fewkes JW (1888) On the development of the calcareous plates of *Asterias*. *Bull Mus Comp Zool* **17**, 1–56.

Fisher WK (1928) Asteroidea of the North Pacific and adjacent waters, Part 2. Forcipulata (Part). *Bull US Natl Mus* **76**, 1–245.

Gale AS (1987a) Phylogeny and classification of the Asteroidea (Echinodermata). *Zool J Linn Soc* **89**, 107–132.

Gale AS (1987b) Goniasteridae (Asteroidea, Echinodermata) from the Late Cretaceous of north-west Europe. The genera *Metopaster* and *Recurvaster*. *Mesoz Res* **1**, 1–69.

Gale AS (1988) Goniasteridae (Asteroidea, Echinodermata) from the Late Cretaceous of north-west Europe. The genera *Callilderma*, *Crateraster, Nymphaster* and *Chomataster*. *Mesoz Res* **1**, 151–186.

Gale AS (2011) The phylogeny of post-Palaeozoic Asteroidea (Neoasteroidea, Echinodermata). *Spec Pap Palaeontol* **85**, 1–112.

Gemmill JF (1912) I. The development of the starfish *Solaster endeca* Forbes. *Trans Zool Soc Lond* **20**, 1–71.

Gemmill JF (1914) The development and certain points in the adult structure of the starfish *Asterias rubens*, L. *Philos Trans R Soc Lond B Biol Sci* **205**, 213–294.

Gemmill JF (1920) Memoirs: the development of the starfish *Crossaster papposus*, Müller and Troschel. *Q J Microsc Sci* **2**, 155.

Gordon I (1929) Skeletal development in *Arbacia*, *Echinarachnius* and *Leptasterias*. *Philos Trans R Soc Lond B* **217**, 289–334.

Hotchkiss FHC (2009) Arm stumps and regeneration models in Asteroidea (Echinodermata). *Proc Biol Soc Wash* **122**, 342–354.

Howell KL, Rogers AD, Tyler PA, et al. (2004) Reproductive isolation among morphotypes of the Atlantic seastar species *Zoroaster fulgens* (Asteroidea: Echinodermata). *Mar Biol* **144**, 977–984.

Janies D (2001) Phylogenetic relationships of extant echinoderm classes. *Can J Zool* **79**, 1232–1250.

Janies DA, Voight JR, Daly M (2011) Echinoderm phylogeny including *Xyloplax*, a progenetic asteroid. *Syst Biol* **60**, 420–438.

Kerkhoff AJ, Enquist BJ (2009) Multiplicative by nature: why logarithmic transformation is necessary in allometry. *J Theor Biol* **257**, 519–521.

Koehler R (1896) Résultats scientifiques de la campagne du Caudan dans de Golfe de Gascogne. Echinodermes. *Annls Univ Lyon* **26**, 33–122.

Komatsu M (1975) On the development of the sea-star, *Astropecten latespinosus* Meissner. *Biol Bull* **148**, 49–59.

Komatsu M, Nojima S (1985) Development of the seastar, *Astropecten gisselbrechti* Doderlein. *Pac Sci* **39**, 274–282.

Komatsu M, Kano YT, Yoshizawa H, et al. (1979) Reproduction and development of the hermaphroditic sea-star, *Asterina minor* Hayashi. *Biol Bull* **157**, 258–274.

Linchangco GV, Foltz DW, Reid R, et al. (2017) The phylogeny of extant starfish (Asteroidea: Echinodermata) including *Xyloplax*, based on comparative transcriptomics. *Mol Phylogenet Evol* **115**, 161–170.

Lopes EM, Ventura CRR (2016) Development of the sea star *Echinaster (Othilia) brasiliensis*, with inference on the evolution of development and skeletal plates in Asteroidea. *Biol Bull* **230**, 25–34.

de Loriol P (1883) Catalogue raisonné des échinodermes recueillis par M.V. de Robillard *à l'ile* Maurice. *Mem Soc Phys Hist Nat Genève* **28**, 1–64.

Mah CL (2000) Preliminary phylogeny of the forcipulatacean Asteroidea. *Am Zool* **40**, 375–381.

Mah CL (2006) Phylogeny and biogeography of the deep-sea goniasterid *Circeaster* (Echinodermata, Asteroidea, Goniasteridae) including descriptions of six new species. *Zoosystema* **28**, 917–954.

Mah C (2007) Phylogeny of the Zoroasteridae (Zorocallina; Forcipulatida): evolutionary events in deep-sea Asteroidea displaying Palaeozoic features. *Zool J Linnean Soc* **150**, 177–210.

Mah CL, Blake DB (2012) Global diversity and phylogeny of the Asteroidea (Echinodermata). *PLoS ONE* **7**, e35644.

Mah C, Foltz D (2011a) Molecular phylogeny of the Forcipulatacea (Asteroidea: Echinodermata): systematics and biogeography. *Zool J Linnean Soc* **162**, 646–660.

Mah C, Foltz D (2011b) Molecular phylogeny of the Valvatacea (Asteroidea: Echinodermata). *Zool J Linnean Soc* **161**, 769–788.

Mah C, Nizinski M, Lundsten L (2010) Phylogenetic revision of the Hippasterinae (Goniasteridae; Asteroidea): systematics of deep sea corallivores, including one new genus and three new species. *Zool J Linnean Soc* **160**, 266–301.

Mah C, Linse K, Copley J, et al. (2015) Description of a new family, new genus, and two new species of deep-sea Forcipulatacea (Asteroidea), including the first known sea star from hydrothermal vent habitats. *Zool J Linnean Soc* **174**, 93–113.

Mooi R, David B (2000) What a new model of skeletal homologies tells us about asteroid evolution. *Am Zool* **40**, 326–339.

Mooi R, David B (2008) Radial symmetry, the anterior/posterior axis, and echinoderm Hox Genes. *Annu Rev Ecol Evol Syst* **39**, 43–62.

Mooi R, David B, Marchand D (1994) Echinoderm skeletal homologies: classical morphology meets modern phylogenetics. *Echinoderms through time*, pp. 87–95. Balkema, Rotterdam.

Mooi R, Rowe F, David B (1998) Application of a theory of axial and extraxial skeletal homologies to concentricycloid morphology. *Echinoderms: San Francisco*, pp. 61–62. Balkema, Rotterdam.

Mortensen T (1921) *Studies of the Development and Larval Forms of Echinoderms*. Copenhagen: Gad.

Müller AH (1961) Zur Kenntnis mesozoischer Asteroidea. *Abh Dtsch Akad Wiss Berl* **1**, 272–282.

Oguro C, Komatsu M, Kano YT (1976) Development and metamorphosis of the sea-star, *Astropecten scoparius* Valenciennes. *Biol Bull* **151**, 560–573.

Okazaki K (1960) Skeleton formation of sea urchin larvae. *Embryologia* **5**, 283–320.

Pernet B, Livingston BT, Sojka C, et al. (2017) Embryogenesis and larval development of the seastar *Astropecten armatus*. *Invertebr Biol* **136**, 121–133.

Perrier E (1881) Description sommaire des espèces nouvelles d'astéries. *Bull Mus Comp Zool* **9**, 1–31.

Perrier E (1885) Première note préliminaire des les échinodermes, recueillis durant les campagnes de dragages sous-marines du Travailleur et du Talisman. *Annls Sci Nat* **22**, 1–72.

Perrier E (1891) Stellérides nouveaux provenant des campagnes du yacht l'Hirondelle. *Mém Soc Zool France* **4**, 258–271.

Rasmussen HW (1950) Cretaceous Asteroidea and Ophiuroidea with a special reference to the species found in Denmark. *Den Geol Unders* **2**, 1–134.

Raup DM (1966) The endoskeleton. In: *Physiology of Echinodermata*. (ed. Boolootian RA), pp. 379–395. New York: John Wiley.

Siddall SE (1979) Development of ossicles in juveniles of the sea star *Echinaster sentus*. *Bull Mar Sci* **29**, 278–282.

Smith AB (1980) Stereom microstructure of the echinoid test. *Spec Pap Palaeontol* **25**, 1–324.

Spencer WK (1913) The evolution of Cretaceous Asteroidea. *Philos Trans R Soc Lond B* **204**, 99–177.

Stricker SA (1985) The ultrastructure and formation of the calcareous ossicles in the body wall of the sea cucumber *Leptosynapta clarki* (Echinodermata, Holothuroida). *Zoomorphology* **105**, 209–222.

Sumida PYG, Tyler PA, Billett DSM (2001) Early juvenile development of deep-sea asteroids of the NE Atlantic Ocean, with notes on juvenile bathymetric distributions. *Acta Zool* **82**, 11–40.

Telford MJ, Lowe CJ, Cameron CB, et al. (2014) Phylogenomic analysis of echinoderm class relationships supports Asterozoa. *Proc R Soc Biol* **281**, 20 140 479.

Thomson CW (1873) *The Depths of the Sea*. London: Macmillan.

Turner RL, Dearborn JH (1972) Skeletal morphology of the mud star, *Ctenodiscus crispatus* (Echinodermata: Asteroidea). *J Morphol* **138**, 239–262.

Verrill AE (1884) Notice of the remarkable marine fauna occupying the outer banks off the southern coast of New England. *Am J Sci* **3**, 213–220.

Verrill AE (1894) Descriptions of new species of starfishes and ophiurans, with a revision of certain species formerly described; mostly from the collections made by the United States Commission of Fish and Fisheries. *Proc US Natl Mus* **17**, 245–297.

Villier L, Blake DB, Jagt JWM, et al. (2004) A preliminary phylogeny of the Pterasteridae (Echinodermata, Asteroidea) and the first fossil record: Late Cretaceous of Germany and Belgium. *Paläont Z* **78**, 281–299.

Villier L, Brayard A, Bylund KG, et al. (2018) *Superstesaster promissor* gen. et sp. nov., a new starfish (Echinodermata, Asteroidea) from the Early Triassic of Utah, USA, filling a major gap in the phylogeny of asteroids. *J Syst Palaeontol* **16**, 395–415.

Supporting Information

Additional Supporting Information may be found in the online version of this article:

Fig. S1 First ambulacrals length, proximal and distal height, according to *R*.

Fig. S2 SEM images of the ossicles of *Pisaster ochraceus* YPM No. 87690 (A, C, F), *Brisingaster robillardi* MNHN-IE-2013-12874 (D, G), and *Neomorphaster forcipatus* YPM No. 87682 (B, E, H).

Table S1 Measures of one first ambulacral of each dissected specimen.

Table S2 Measurements of ambulacrals in actinal view.

Table S3 Measurements of the seven dissected specimens (see Table 1 for collection numbers of Z1–Z7), plus 24 individuals (originally from the batch MNHN-IE-2013-12853).